Reply to the comments of Referee #1 (F. Livio)

REVIEWER:

General comments

Boncio et al. propose a statistical analysis of the surface rupture distribution and an evaluation of the most probable width of surface rupture, occurring during thrust earthquakes. This approach, used for probabilistic fault hazard assessment of distributed faults, is a well-established practice previously performed mainly using strike slip and normal faults datasets. A systematic data review for thrust faults alone was still lacking in literature (partially made on Japanese earthquakes) a thus this work present a novelty aspect that must be considered. The approach is similar to previous studies and no particularly innovations have been proposed from the methodological point of view. An adequate discussion on fold-related faults (i.e., flexural slip faults and bending-moment faults) has been introduced even if I would have found interesting a statistical approach also on these structures (see below) – even to exclude that a PDF can be invoked for their distribution in space. In summary, I found this work a first interesting (and necessary) review of some well-documented case studies of thrust surface faulting. These observations are resulting in a first proposal of setback distances from fault traces, that should be taken into considerations for siting purposes and by public administrations providing guidelines for land-planning. Nevertheless, some major revisions should be made. In the following, some specific scientific issues are opened to the discussion (Specific Comments) and several notes are made (technical corrections).

Scientific Comments

1) *Firstly, I strongly suggest the Authors to add as supplementary Material the georeferenced maps they used. Ideally, the trace of the main and distributed faults could be provided, as georeferenced shapefiles or .kmz files. This could provide the original datasets that can be used by other scientists for further analysis, data checking etc. and it is one of the main objective of this kind of "data mining" papers. At the moment, no further inspection on the used dataset can be made and this is one of the major faults of the paper in the present form.*

2) *A note on the methodological approach used for measuring distances. The approach depicted in Figure 1 could result in some biased measurements In fact, it is depending on the azimuth of the main fault strike, in turn derived from the chosen fault tips, fault segmentation etc. This is working well for distributed fault striking parallel to the main one but can be misleading for non-parallel faults. Why not to use a GRID-based approach (like in Petersen al. or in Youngs et al.)? This would also assure data comparison with previous works.*

3) *At lines 167 – 173 some characteristics of the bending moment faults (BMF), significantly contributing in widening the WRZ, are described. Regarding this point, wavelenght of the thrust-related fold can be considered in order to recognized distant ruptures due to BMF but has not to be taken alone: these secondary structures a more related to hinge zones (and thus geometric characteristics of the fold i.e., curvature of the fold, thickness of the folded single-layer etc.) than to wavelength alone. Distances proposed to distinguish between pressure ridge anticline vs larger scale structures are just cutoff distance not discussed in their significance. Moreover, I find hard to distinguish between the two of them at intermediate scale. I think that the choice to exclude these structures from a probabilistic analysis can be right but further discussion or objective criteria are needed in order to correctly hierarchize thrust-related faults. Some attempts can be made considering structurally derived cutoff distances: e.g., depth of the sole of the thrust, axial planes (i.e. possible hinge zones) predicted by kink band modeling, etc. In any case, the Authors*

should provide schematic cross-sections of the considered case studies presenting BMF, so that a direct comparison can be made with the schemes in Figure 2.

4) *The best probability density function (PDF) of the distributed faults has been obtained through a commercial software (lines 174-177) but no detailed information is available on the procedure of fitness testing used by the software (a Kolmogorov-Smirnov test is cited but no scores are reported). Maybe this information should be provided as Supplementary Material. A quantitative comparison of the different tested PDF should be provided. Did you test only unimodal distribution or also multimodal? Did you tried to include also bending-moment and flexural-slip faults and fit the entire dataset with a multimodal PDF? Very few people know the Birbaum-Saunders distribution (originally thought to predict the life of mechanical parts subject to stress before failure). Some consideration should be made on the chosen PDF. I found that the statistical analytics are not well explained in the present form of the text and that maybe some other ways of data fitting should have been tested. Lines 185-197 (Figure 4) briefly describe the trend of the fitted PDF considering distances corresponding to progressively increasing cumulative probabilities of occurrence. Here, a strong statistical approach is lacking in transforming cumulative probabilities in distances proposed for setback etc. a qualitative approach is used. The Authors state that "90% probability : : :seems to be a reasonable value to cut the outliers" (line 185-186) and ": : :40% probability bounds reasonably well the zone where the most of the ruptures occur". These statements are not quantitively constrained. If you use a PDF like the Birbaum-Saunders, that can be characterized by a strong skewness and a long right tail, maybe outliers have to be evaluated with cautiousness. Vanegas, L. H., Rondón, L. M., & Cysneiros, F. J. A. (2012). Diagnostic procedures in Birnbaum–Saunders nonlinear regression models. Computational Statistics & Data Analysis, 56(6), 1662-1680. Provide a review of the tests that can be performed of this PDF in order to identify outliers.*

MINOR POINTS
Lines 88-93: here, a brief summary of the main pertaining references is given. I suggest to add the following work: - Takao, M., Annaka, T., Kurita, T., 2013. Application of probabilistic fault displacement hazard analysis in Japan. J. Jpn. Assoc. Earthquake Eng. 13 (1), 17–36.
Line 249: "and parallel to the anticline hinge"; it depends: not e.g., in transpressive settings.
Line 201: "total width": do you mean maximum? Or average?
Line 202: did you tried plotting net slip instead of vertical component? Maybe the median of the width could be more clustered. Data on Figure 5 are quite scattered, maybe a bilinear upper bound can be proposed with a flat top toward the right.
Line 204-205: also this part is questionable. If we admit that a positive upper bound can be supposed in the lower left of the graph (i.e., less than 200 m) how do you explain this threshold distance? Intercept point to ca. 20 m of width, independent from the displacement on the main fault. How do you comment this? It is and expression of aleatory uncertainty or rather related to a geologic process? In any case this result is really important!
Line 252: "first order stiffness of the folded material". I don't get the point. What's a "first order stiffness"? are you referring to tensile strength or other mechanical properties of the upper layers? Please, discuss this point or rather avoid this sentence that can be misleading.
Line 268-269: "cold criteria" is not appropriate. Do you mean objective? Threshold values?

TECHNICAL CORRECTIONS

Abstract should be considerably shortened. I would put a major stress on the major advances of this work and novelty, in the first paragraphs.
Line 58: put AP Act in refs
Line 131: suggested change – ": : :faults (type i) are reverse faults: : :" Table 1: indicate also the mapping scale of each digitized ma
Figure 3: should be a little bit improved both in the graphing type and in the format. A vectorial image should work best.
Figure 4: alpha and beta parameters of the chosen PDF are not discussed in the text or in the caption. Some additional information should be provided and discussed: e.g.., both hangingwall and footwall datasets show similar alpha values but different beta (i.e. median) parameters.
RESPONSE:
We would like to thank the reviewer for the appropriate comments and very useful suggestions. We considered all the comments in the revised version of the manuscript.
The queries to the scientific comments have been answered separately in the following section.
All the minor points and technical corrections suggested by the Referee were taken into account.

SCIENTIFIC COMMENTS

1) *Firstly, I strongly suggest the Authors to add as supplementary Material the georeferenced maps they used. Ideally, the trace of the main and distributed faults could be provided, as georeferenced shapefiles or .kmz files. This could provide the original datasets that can be used by other scientists for further analysis, data checking etc. and it is one of the main objective of this kind of "data mining" papers. At the moment, no further inspection on the used dataset can be made and this is one of the major faults of the paper in the present form.*

RESPONSE: We added electronic supplementary material, consisting in a summary table with all the measured data and several maps, one for every earthquake, showing the measurement details and the chosen average strike of the main fault.

2) *A note on the methodological approach used for measuring distances. The approach depicted in Figure 1 could result in some biased measurements In fact, it is depending on the azimuth of the main fault strike, in turn derived from the chosen fault tips, fault segmentation etc. This is working well for distributed fault striking parallel to the main one but can be misleading for non-parallel faults. Why not to use a GRID-based approach (like in Petersen al. or in Youngs et al.)? This would also assure data comparison with previous works.*

RESPONSE: We think our approach is more detailed than that used by Petersen et al. (2011) (we used closely spaced measurements). We will explain better the method in the text.
In any case, independently from the used method, we need to define the azimuth along which the distance from the main fault is measured. One target of the paper is zoning the hazard around a mapped fault. Therefore, we need distances from the fault trace. We were careful in defining the measurement azimuth, taking into account the variations in strike of the main fault, and avoiding duplication of measurements. The maps added in the auxiliary material will help the reader in judging our choices.

3) *At lines 167 – 173 some characteristics of the bending moment faults (BMF), significantly contributing in widening the WRZ, are described. Regarding this point, wavelenght of the thrust-related fold can be considered in order to recognized distant ruptures due to BMF but has not to be taken alone: these secondary structures a more related to hinge zones (and thus geometric characteristics of the fold i.e., curvature of the fold, thickness of the folded single-layer etc.) than to wavelength alone. Distances proposed to distinguish between pressure ridge anticline vs larger scale structures are just cutoff distance not discussed in their significance. Moreover, I find hard to distinguish between the two of them at intermediate scale. I think that the choice to exclude these structures from a probabilistic analysis can be right but further discussion or objective criteria are needed in order to correctly hierarchize thrust-related faults. Some attempts can be made considering structurally derived cutoff distances: e.g., depth of the sole of the thrust, axial planes (i.e. possible hinge zones) predicted by kink band modeling, etc. In any case, the Authors should provide schematic cross-sections of the considered case studies presenting BMF, so that a direct comparison can be made with the schemes in Figure 2.*

RESPONSE: We analyzed the data both with and without BMF and F-S secondary ruptures (two different PDFs). We also differentiated Sympathetic ruptures (Sy). In general, in the revised version of the manuscript we tried to discuss more clearly all the points suggested by the Referee.

4) *The best probability density function (PDF) of the distributed faults has been obtained through a commercial software (lines 174-177) but no detailed information is available on the procedure of fitness testing used by the software (a Kolmogorov-Smirnov test is cited but no scores are reported). Maybe this information should be provided as Supplementary Material. A quantitative comparison of the different tested PDF should be provided. Did you test only unimodal distribution or also multimodal? Did you tried to include also bending-moment and flexural-slip faults and fit the entire dataset with a multimodal PDF? Very few people know the Birbaum-Saunders distribution (originally thought to predict the life of mechanical parts subject to stress before failure). Some consideration should be made on the chosen PDF. I found that the statistical analytics are not well explained in the present form of the text and that maybe some other ways of data fitting should have been tested. Lines 185-197 (Figure 4) briefly describe the trend of the fitted PDF considering distances corresponding to progressively increasing cumulative probabilities of occurrence. Here, a strong statistical approach is lacking in transforming cumulative probabilities in distances proposed for setback etc. a qualitative approach is used. The Authors state that "90% probability : : :seems to be a reasonable value to cut the outliers" (line 185-186) and ": : :40% probability bounds reasonably well the zone where the most of the ruptures occur". These statements are not quantitively constrained. If you use a PDF like the Birbaum-Saunders, that can be characterized by a strong skewness and a long right tail, maybe outliers have to be evaluated with cautiousness. Vanegas, L. H., Rondón, L. M., & Cysneiros, F. J. A. (2012). Diagnostic procedures in Birnbaum–Saunders nonlinear regression models. Computational Statistics & Data Analysis, 56(6), 1662-1680. Provide a review of the tests that can be performed of this PDF in order to identify outliers.*

RESPONSE: The aim is to find PDFs only based on their ability to fit the data. In order to find these PDFs in the easiest way the possible, we decided to use a commercial software, assuming that the software is working sufficiently well. We think that a deep statistical analysis of the data is very interesting, but beyond the aim of this paper.

Concerning the percentiles used for sizing the zones, we acknowledge that they are subjective choices. In the revised version we stated more clearly that these are subjective choices. We think that it is very difficult to define really objective criteria. We also think that the reader can accept our suggestions as an “expert judgement” or, most importantly, can make its own choice.

Reply to the comments of Referee #2

REVIEWER

General comments

The MS represents a substantial contribution to mitigation of surface faulting hazard, which falls into the scope of NHESS. The paper uses existing worldwide datasets to propose easily applicable criteria to mitigate the surface displacement hazard that can occur during earthquakes. The authors statistically process worldwide data to define "setback" zones as avoidance or warning zones for human occupancy facilities. According to my knowledge, this approach is innovative. Usually, statistics on datasets are used in Fault Displacement Hazard for deriving prediction equations (probability of rupture, attenuation of displacement with distance), but my feeling is that this work is an appropriate and valid way to treat the problem. An interesting outcome is that the statistics tend to confirm part of the Italian regulation lines, but on the other hand the results suggest that the avoidance should be increased for well-mapped cases. I find the discussion on Bending-Moment and Flexural-Slip ruptures a bit disappointing (see below). Also, the proposed conclusion is more an abstract and I would expect some perspectives to the work that has been done (see below). The MS is clear and concise; contents are well exposed and structured, easy to understand for a wide audience. Figures are good, except the Figure 4 where labels are too small. English is clear to me (English is not my native language). Figures are generally relevant, but I wonder if the Figure 2 (Scarp classification) is really helpful. I suggest to the authors to include in Supplementary Material the rupture maps which would (probably) help the reader to understand some choices about calculation of distances, definition of "average MF direction", etc (see below). The title and abstract clearly and unambiguously reflect the contents of the paper. The authors use an adequate number and quality of accessible references, from which they extract a fair and relevant content. Therefore, I would suggest that Scientific Significance and Quality are good and Presentation Quality is very good (even if some minor corrections would improve the MS). To me, the MS would be accepted after some revision such as follows.

MAJOR ISSUES AND RECOMMENDATIONS

1. *My first comment concerns the Bending-Moment and Flexural Slip ruptures (distributed deformation features). The authors do not consider these in their analysis because "strictly related to the structural setting of the area (presence and wavelength of the fold". I don't really understand this statement because each rupture, its splays, its pattern of surface deformation is somehow related to a specific structural pattern (geometry of the fault at depth, segmentation, local arrangement of rock packs, etc). Maybe the authors have in mind the fact that BM and FS are rather related to Coseismic folding (ductile deformation) during earthquake than to Coseismic propagation of the rupture plane to the ground surface? I would suggest to the authors to discuss the way these BM and FS distributed ruptures could be accounted for: this is a critical issue for Italy where thrust-related earthquakes usually occur on blind faults and BM and FS on associated fold are the actual main hazard. In section 3, line 173, the authors seem to mean that there is a direct relation between fold wavelength and location of BM-FS ruptures: this could be a proxy and a way to map and define "Warning or Susceptible zones" to include them in zoning. In line 245-246, the authors write that the*

"knowledge of the structural setting of the area help in identifying zones potentially susceptible to BM and FS faulting", then why not suggest that such structural features (active folds associated with a thrust) could be defined as "Susceptible Zones"?

2. *My second comment deals with the definition of metrics and the chosen hypotheses to calculate distances between secondary ruptures and main ruptures. The Figure 1 presents the approach considering a quite simple case, where the "average MF direction" is easy to infer. It is not clear to me how the authors would cope with curved and/or discontinuous ruptures and scarps; at which scale does the average trace is designed? This would change depending on the rupture size (ex. 240 km of Wenchuan vs 15 km of San Fernando). The MS would largely benefit from the inclusion of the rupture maps, so that the reader would understand the authors' method and eventually reproduce the method to improve their work in further steps. Other questions arise for this point: for instance, how the authors measured the distance of secondary ruptures at the tip of the fault, out of the main trace?*

3. *Third comment. The results in terms of statistical outcomes are sufficient to support the conclusions (i.e. definition of three different levels of zones). However, I find the section "Conclusions" look like an Abstract. They should include some perspective or prospective insights, like for instance: - How to take the BM and FS ruptures into account? - Do we need more data to build more robust zoning results? – Would this work or compiled database useful in Probabilistic approach of Fault Displacement Hazard Analysis? - Could future similar developments be applied to other tectonic and permanent deformation features like folding, tilting, extensional/compressional strain (see discussions in ANSI/ANS-2.30-2015 Criteria for Assessing Tectonic Surface Fault Rupture and Deformation at Nuclear Facilities)?*

SPECIFIC POINTS

Replace "associated to" by "associated with" or "related to"

Lines 50 51 – Define "main fault" and "secondary faulting"

Line 63 - Ambiguous statement: "The AP act defines a minimum distance (: : :) within which critical facilities and structures designed for human occupancy cannot be built". Delete "Critical facilities" because AP Act is only for housing.

Line 68 – Please specify which facilities are concerned by "land management" term: only housing, or also lifelines, pipelines, storages or other facilities

Line 73 – The fault zones' widths vary at different Levels instead of The fault zones vary at different Levels

Line 82 – Please explain what is decided when the "Susceptible Zone" is defined: Avoidance?

Line 88 – Rephrase "In general, worldwide the width of the rupture zone : : :"

Lines 92 to 95 – Sentence is to be rephrased. Ambiguous sentence: "1: to collect the data from well-studied (: : :) earthquakes" is not exactly was has been done. Instead, it is a compilation of surface maps and displacement observations, not a collection of data (in the field).

Lines 117 to 129 - after reading the whole paper, I am not really sure that this description of scarp classification and related section is useful. What is finally used in the conclusions? The authors may earn space here.

Lines 135-136 - clarify whether the scarps are described according to the same classification in the references. Or is it a re-interpretation based on drawings, map?

Line 142 – The collected data were instead of The collected data was

Lines 154 and 155 – The sentence suggests that there is surface geology information in the references: is that the case or is this an assumption?

Line 162 - Subsurface data give indication of the location of an anticline on top of the fault: where are located the FS ruptures with respect to this fold?

Lines 168-169 – "the distribution of the BM faults for the El Asnam earthquake is very similar to the distribution of extensional ruptures for the San Fernando earthquake": please provide an explanation to this surprising statement. Is there a similar wavelength of associated fault? So no dependence on magnitude (7.3 against 6.6)?

Line 182 – Please explain the Kolmogorov-Smirnov test (if you decide to mention it), its specificity and the reason why it has been selected. Otherwise, you can skip this information.

Line 186 – Explain why "the 90% probability (: : :) seems to be a reasonable value to cut the outliers": for statistical reasons considering the examined population? Or because its outcome in terms of setback size fits with an a priori?

Line 204 – "the data with BM and FS faults are excluded" instead of "the data with BM and FS faults is excluded"

Line 209-210 – "the maximum WRZ, including the secondary ruptures away from the main fault, can be up to 200 m or wider": did you explore if there is a relation between this max. width and the earthquake magnitude?

Lines 221 to 225 – I would suggest to moderate this with the conclusion coming from the MB and FS analysis. In cases of verified active folds (related to thrusts), this conclusion should be revised, especially for Italy where most of the thrusts are blind (Po Plain) and could cause folding and BM-FS ruptures at the surface as the major hazard.

Line 234 – "Assuming that this relation is robust enough" instead of "Assuming that this relation is real" would be better, I think

Line 248 – I was wondering if any BM reverse faulting has never been observed in the synclinal axis. This part requires more perspective. How can we account for these ruptures? Any recommendation?

Line 282 – This confirms that the avoidance zone should be larger" would be more appropriate than "This suggests that the avoidance zone should be larger" Table 1 - Why 2014 Nagano earthquake rupture has not been included? Figure 1 - There is a different approach for short, intermediate and long secondary ruptures in measuring distance to main fault. Explain please. Caption - Main fault: How is defined main fault? Max. displacement? On the map, this "main fault" runs along the base of the scarp I presume. In complex cases like (d), (e), (f), Main fault trace is traced along the free face or along the more external topographic bulge? Figure 2 – Explain where the Main fault would be mapped on Figure 1 on each case.

RESPONSE: We would like to thank the reviewer for the appropriate and very useful comments and suggestions. We considered all the comments in the revised version of the manuscript.

The Reviewer's major issues and recommendations have been replied in the following section. All the specific points and minor corrections suggested by the Referee were taken into account.

MAJOR ISSUES AND RECOMMENDATIONS

1. *My first comment concerns the Bending-Moment and Flexural Slip ruptures (distributed deformation features). The authors do not consider these in their analysis because "strictly related to the structural setting of the area (presence and wavelength of the fold". I don't really understand this statement because each rupture, its splays, its pattern of surface deformation is somehow related to a specific structural pattern (geometry of the fault at depth, segmentation, local arrangement of rock packs, etc). Maybe the authors have in mind the fact that BM and FS are rather related to Coseismic folding (ductile deformation) during earthquake than to Coseismic propagation of the rupture plane to the ground surface? I would suggest to the authors to discuss the way these BM and FS distributed ruptures could be accounted for: this is a critical issue for Italy where thrust-related earthquakes usually occur on blind faults and BM and FS on associated fold are the actual main hazard. In section 3, line 173, the authors seem to mean that there is a direct relation between fold wavelength and location of BM-FS ruptures: this could be a proxy and a way to map and define "Warning or Susceptible zones" to include them in zoning. In line 245-246, the authors write that the "knowledge of the structural setting of the area help in identifying zones potentially susceptible to BM and FS faulting", then why not suggest that such structural features (active folds associated with a thrust) could be defined as "Susceptible Zones"?*

RESPONSE: We fully understand the Reviewer's criticism. In fact, the most correct approach for considering secondary faulting (particularly ruptures very far from MF) is a difficult task. Basically, our aim in the paper is to distinguish, if feasible, secondary ruptures that occur in a rather "systematic" way compared to the main fault (i.e., only related to the propagation of the main rupture up to the surface), called "simple thrust ruptures", from secondary ruptures that can be affected by structural features that are not systematic (large-scale folds, lithology of folded rocks, …). We discussed this point more deeply and more clearly.

Most importantly, we decided to analyze the data both with and without B-M and F-S distributed ruptures (two different PDFs), and we discussed the results and the possible implications. We also distinguished sympathetic ruptures (Sy). Therefore, we think the paper will be largely improved from this point of view.

2. *My second comment deals with the definition of metrics and the chosen hypotheses to calculate distances between secondary ruptures and main ruptures. The Figure 1 presents the approach considering a quite simple case, where the "average MF direction" is easy to infer. It is not clear to me how the authors would cope with curved and/or discontinuous ruptures and scarps; at which scale does the average trace is designed? This would change depending on the rupture size (ex. 240 km of Wenchuan vs 15 km of San Fernando). The MS would largely benefit from the inclusion of the rupture maps, so that the reader would understand the authors' method and eventually reproduce the method to improve their work in further steps. Other questions arise for this point: for instance, how the authors measured the distance of secondary ruptures at the tip of the fault, out of the main trace?*

RESPONSE: We have added electronic supplementary material, consisting in a summary table with all the measured data and several maps, one for every earthquake, showing the measurement details, including the chosen average strike of the main fault. Moreover, we explained better the method in the text.

In general, we were careful in defining the average strike of the MF and the measurement azimuths, taking into account the variations in strike of the main fault (only first-order, kms-scale strike variations have been considered), and avoiding duplication of measurements. The maps of the auxiliary material will help the reader in judging our choices.

We also added data from the Nagano 2014 earthquake, as suggested.

3. *Third comment. The results in terms of statistical outcomes are sufficient to support the conclusions (i.e. definition of three different levels of zones). However, I find the section "Conclusions" look like an Abstract. They should include some perspective or prospective insights, like for instance: - How to take the BM and FS ruptures into account? - Do we need more data to build more robust zoning results? – Would this work or compiled database useful in Probabilistic approach of Fault Displacement Hazard Analysis? - Could future similar developments be applied to other tectonic and permanent deformation features like folding, tilting, extensional/compressional strain (see discussions in ANSI/ANS-2.30-2015 Criteria for Assessing Tectonic Surface Fault Rupture and Deformation at Nuclear Facilities)?*

RESPONSE: We considered this good suggestion.

Width of surface rupture zone for thrust earthquakes. Implications for earthquake fault zoning.

Paolo Boncio[1], Francesca Liberi[1], Martina Caldarella[1], Fiia C.Nurminen[2]

[1]CRUST-DiSPUTer,“G. D’Annunzio” University of Chieti-Pescara, Chieti, I-66100, Italy

[2]Oulu Mining School, University of Oulu, Oulu, FI-90014, Finland

Correspondence to: Paolo Boncio (paolo.boncio@unich.it)

Abstract. The characteristics of the zones of coseismic surface faulting along thrust faults are analysed in order to define the criteria for zoning the Surface Fault Rupture Hazard (SFRH) along thrust faults. Normal and strike-slip faults have been deeply studied by other authors~~in the past~~ concerning the SFRH, while thrust faults have not been studied with comparable attention.

Surface faulting data were ~~collected from~~compiled for ~~10~~ 11 well-studied historic thrust earthquakes occurred globally (5.4 ≤ M ≤ 7.9). Several different types of coseismic fault scarps characterise the analysed earthquakes, depending on the topography, fault geometry and near-surface materials (simple and hanging wall collapse scarps; pressure ridges; fold scarps and thrust or pressure ridges with bending-moment or flexural-slip secondary faults due to large-scale folding). For all the earthquakes, the distance of ~~secondary~~ distributed ruptures from the ~~main~~ principal fault rupture (r) and the width of the rupture zone (WRZ) were compiled directly from the literature or measured systematically in GIS-georeferenced published maps.

Overall, surface ruptures can occur up to large distances from the main fault (~~~750~~ 2,150 m on the footwall and ~~~1,6~~3,100 m on the hanging wall). Most of them occur on the hanging wall, preferentially in the vicinity of the ~~main~~ principal fault trace (≥ 50% at distances <~ ~~50~~ 250 m). The widest WRZ are recorded where sympathetic slip (Sy) on distant faults occurs, and/or where bending-moment (B-M) or flexural-slip (F-S) ~~secondary~~ fault ruptures, associated ~~to~~ with large-scale folds (hundreds of meters to kilometres in wavelength), are present.

A positive relation between the earthquake magnitude and the total WRZ is evident, while a clear correlation between the vertical displacement on the principal fault and the total WRZ is not found.

The distribution of surface ruptures is fitted with probability density functions, in order to define a criterion to remove outliers (e.g. 90% probability of the cumulative distribution function) and define the zone where the likelihood of having surface ruptures is the highest. This might help in sizing the zones of SFRH during seismic microzonation (SM) mapping.

In order to shape zones of SFRH, a very detailed earthquake geologic study of the fault is necessary (the highest level of SM, i.e., Level 3 SM according to Italian guidelines). In the absence of such a very detailed study (basic SM, i.e., Level 1 SM of Italian guidelines) a width of ~465 840 m (90% probability from “simple thrust” database of distributed ruptures, excluding B-M, F-S and Sy ruptures) seems is suggested to be adequatesufficiently precautionary. For more detailed level SM, where the fault is carefully mapped, one must consider that the highest SFRH is concentrated in a narrow zone, ~60 monly 50-70 in width , that should be considered as a fault avoidance zone (40-50%more than one third of the total distributed ruptures are expected to occur within this zone).

A broad positive relation between the displacement on the main fault and the total width of the rupture zone is found only close to the main fault (total WRZ ≤ 60 m). The total WRZ appears to increase with displacement, from a minimum of nearly 20-30 m for decimetric vertical displacement up to 50-60 m for vertical displacement close to 2 m.

The fault rupture hazard zones should be asymmetric compared to the trace of the main principal fault. The average footwall to hanging wall ratio (FW: HW) is close to 1:2.

These criteria are applicable to “simple thrust faults” faults, without considering possible B-M or F-S secondary fault ruptures on due to large-scale foldsfolding, and without considering sympathetic slip on distant faults. Zones Areas potentially susceptible to B-M or F-S secondary fault ruptures should have their own zones of fault rupture hazard that can be inferred defined by detailed knowledge of the structural setting of the area (shape, wavelength, tightnessgeometry, wavelength and lithology of the thrust-related large-scale folds) and by geomorphic evidence of past secondary faulting. Distant active faults, potentially susceptible to sympathetic triggering, should be zoned as separate principal faults.

The entire database of distributed ruptures (including B-M, F-S and Sy fault ruptures) can be useful in poorly-known areas, in order to assess the extent of the area within which potential sources of fault displacement hazard can be present.

Commento [UW1]: Comment 3 of Rev. 2

The results from this study and the database made available as supplementary material can be used for improving the attenuation relationships for distributed faulting, with possible applications in probabilistic studies of fault displacement hazard.

Key words

Fault rupture hazard, thrust earthquakes, earthquake fault zoning.

1 Introduction

Coseismic surface ruptures during large earthquakes might produce damage to buildings and facilities located on or close to the trace of the active seismogenic fault. This is known as Surface Fault Rupture Hazard (SFRH), a localized hazard that could be avoided if a detailed knowledge of the fault characteristics is achieved. The mitigation of SFRH can be faced by strategies of fault zoning and avoidance or, alternatively, by (or together with) probabilistic estimates of fault displacement hazard (e.g. Youngs et al., 2003; Petersen et al., 2011). Both strategies need to employ, as accurately as possible, the location of the active fault trace, the expected displacement on the ~~main~~ principal fault (i.e. *principal faulting* in Youngs et al., 2003; see below for the definition), the deformation close to the ~~main~~ principal fault, and the distribution of ~~secondary~~ other faulting and fracturing away from it (i.e. *distributed faulting* in Youngs et al., 2003; see below for the definition). While the general ~~fault~~ geometry and the expected displacement of the principal fault can be obtained through a detailed geological study and the application of empirical relationships (e.g. Wells and Coppersmith, 1994), the occurrence of ~~secondary~~ distributed faulting close to and away from the ~~main~~ principal fault rupture is particularly difficult to predict, and only direct observations from well-documented case studies may provide insights on how ~~secondary~~ distributed faulting is expected to occur (e.g. shape and size of rupture zones, attenuation relationships for ~~secondary~~ distributed faulting).

A reference example of fault zoning strategy for mitigating SFRH is the Alquist-Priolo Earthquake Fault Zoning Act (A-P Act), adopted by the state of California (USA) in 1972 (e.g. Bryant and Hart, 2007). The A-P Act defines regulatory zones around active faults (Earthquake Fault Zones, EFZ), within which detailed geologic investigations are required prior to build structures for human occupancy. The boundaries of the EFZ are placed 150-200 m away from the trace of major active faults, or 60 to 90 m away from well-defined minor faults, with exceptions where faults are complex or not vertical. Moreover, the A-P Act defines a minimum distance of 50 feet (15 m) from the well-defined fault trace within which ~~critical facilities and~~ structures designed for human occupancy cannot be built (fault setback), unless proven otherwise. Similarly ~~to the setback of the A-P Act~~, the New Zealand guidelines for development of land on or close to active faults (Kerr et al., 2003) define a fault avoidance zone to ensure life safety. Fault avoidance zones on district planning maps will allow a council to restrict development within the fault avoidance zone and take a risk-based approach to development in built-up areas. The risk-based approach combines the key elements of fault recurrence interval, fault complexity and building importance category. The guidelines recommend a minimum buffer of 20 m either sides of the known fault trace (or the likely rupture zone), unless detailed fault studies prove that the deformed zone is less than that.

Recently, in Italy the Department for Civil Protection published guidelines for land management in areas affected by active and capable faults. For the purpose of the guidelines, an active and capable fault is defined as a fault with demonstrated evidence of surface faulting during the last 40,000 years (Technical Commission for Seismic Microzonation, 2015; SM Working Group, 2015). The guidelines are a tool for zoning active and capable faults during seismic microzonation (SM). They also contain a number of recommendations to assist land managers and planners. The fault zones vary at different Levels of SM. In the basic SM (Level 1 SM according to SM Working Group, 2015), the active fault is zoned with a wide Warning Zone that is conceptually equivalent to the EFZ of the A-P Act. The zone should include all the reasonable inferred fault-rupture hazard of both the ~~main~~ principal fault and other secondary faults, and should account for uncertainties in mapping the fault trace. The guidelines recommend a width of the Warning Zone to be 400 m. Within the Warning Zone, the most detailed level of SM (Level 3 SM) is recommended; this should be mandatory before new development~~construction~~. Level 3 SM implies a ~~very~~ detailed earthquake geology study of the fault. After completing that study, a new, more accurate fault zoning is achieved. This includes a 30 m-wide Fault Avoidance Zone around the accurately-defined fault trace. If some uncertainties persist after Level 3 studies, such as uncertainties about fault trace location or about the possibility of secondary faulting away from the ~~main~~ principal fault, the guidelines suggest the use of a wider zone called Susceptible Zone, within which development is restricted. Uncertainties within the Susceptible Zone can be reduced by additional site-specific investigations. The guidelines recommend a width of the Susceptible Zone to be 160 m, but the final shape and size of the zone depend on the local geology and the level of accuracy reached during Level 3 SM studies. Both Fault Avoidance and Susceptible Zones can be asymmetric compared with the main fault trace, with recommended footwall to hanging wall ratios of 1:4, 1:2 and 1:1 for normal, thrust and strike-slip faults, respectively.

Shape and width of the zones in the Italian guidelines are based mostly on data from normal faulting earthquakes (e.g. Boncio et al., 2012). In general, ~~worldwide the width of the rupture zone (WRZ) for~~ the fault displacement hazard ~~normal~~of normal and strike-slip ~~earthquakes~~ faults (e.g. Youngs et al., 2003; Petersen et al., 2011) ~~is~~ has been much more studied than that of ~~for~~ thrust faults~~earthquakes~~. Zhou et al. (2010) analysed the width of the surface rupture zones of the 2008 Wenchuan earthquake focusing on the rupture zone close to the ~~main~~ principal fault, with implications on the setback distance. However, to our knowledge, a global data ~~collection~~ compilation from well-documented surface thrust faulting earthquakes aimed at analysing the characteristics of the WRZ is lacking in the scientific literature.

The objectives of this work are: 1) to ~~collect the~~compile data from well-studied surface faulting thrust earthquakes globally (we analysed ~~10~~ 11 earthquakes with magnitudes ranging from 5.4 to 7.9); 2) to analyse statistically the distribution of surface ruptures compared to the ~~main~~ principal fault and the associated WRZ; and 3) to compare the results with the ~~contemporary~~ Italian guidelines and discuss the implications for earthquake fault zoning.

2 Methodology

This work analyses the data from ~~10~~ 11 well-studied historic surface faulting thrust earthquakes occurred worldwide during the last few decades (Table 1). These historic earthquakes range in magnitude (Mw) from 5.4 to 7.9 and belong to different tectonic settings, such as continental collision (Spitak, 1988; Kashmir, 2005; Wenchuan, 2008), fold-and-thrust belt (El Asnam, 1980), oceanic-continental or continental-continental collision in large-scale subduction systems (Chi-Chi, 1999; Nagano, 2014), transform plate boundary (San Fernando, 1971; Coalinga-Nunez, 1983) and intraplate regions (Marryat Creek, 1986; Tennant Creek, 1988; Killari, 1993).

We compiled from the literature data on both principal and distributed faulting, as defined by Youngs et al. (2003). Principal faulting is displacement along the main fault responsible for the release of seismic energy during the earthquake. At the surface, the displacement may occur along a single narrow trace of the principal fault or within a meters-scale wide fault zone. Distributed faulting is displacement on other faults in the vicinity of the principal fault rupture. Distributed ruptures are often discontinuous and may occur tens of meters to kilometers away from the principal fault rupture. Displacement may occur on secondary faults connected with the principal fault, such as splay faults, or on pre-existing faults structurally unconnected with the main fault (called here sympathetic fault ruptures). In particular, f~~F~~or the purpose of this work, the following parameters were ~~collected~~ extracted from the literature listed in Table 1: i) displacement (vertical, horizontal and net slip, if available) on the ~~main~~ principal fault rupture and coordinates of the referred measurement points for strands of the principal fault having associated distributed ruptures; ii) distance from the ~~main~~ principal fault to the ~~secondary~~ distributed ruptures (r in Fig. 1), distinguishing between the ones on hanging wall and on footwall; iii) displacement on distributed ruptures ~~secondary faults~~ (if available); iv) width of the rupture zone (WRZ), distinguishing between the ones on hanging wall and on footwall; and v) scarp type (Fig. 2).

Commento [UW2]: Comments from Rev. 2

When available, the surface rupture data was ~~collected~~ compiled directly from ~~the literature~~published tables (e.g., Chi-Chi, 1999; Wenchuan, 2008), but in most of the other cases the rupture data was measured from the ~~published~~ maps published by the previous authors that were GIS-georeferenced for the purpose of this work. Figure 1 displays the technique used for measuring the distance between the ~~main~~ principal fault rupture (PF) and the ~~secondary~~ distributed ruptures (DR), which allowed us to sample the rupture zone systematically and in reasonable detail. The measurements carried out on the published maps are illustrated in Fig.s S1 to S11 of the online supplementary material, and the entire compiled database is made available in Table S1. The accuracy of the measurements depends on the scale of the original maps and on the level of detail reported in the maps (the original scale of the published maps is reported in the figures of the supplementary material). In this work only detailed maps were considered, and uncertain or inferred ruptures were not taken into account. It is important to specify that the database made available in Table S1 of the supplementary material can be used only for analysing distributed faulting. Data on the principal fault rupture are not complete, because the strands of the principal fault without distributed ruptures were not considered.

Commento [UW3]: Comments 1 and 2 of Rev. 1 and Comment 2 of Rev. 2

In order to distinguish the principal fault rupture from distributed ruptures, all of the following were considered: 1) larger displacement compared to distributed faulting; 2) longer continuity; 3) coincidence or nearly coincidence with major tectonic/geomorphologic features, such as the trace of the main fault mapped before the earthquake on geologic maps.

The distance was measured perpendicularly to the average direction of the principal fault, which was defined by visual inspection of the published maps, averaging the direction of first-order sections of the principal fault rupture (few to several km-long). Particular attention was paid close to variations of the average strike, in order to avoid duplicate measurements. In some places, the principal fault rupture is discontinuous. In few of those cases, and only for the purpose of measuring the distance of distributed ruptures from the main fault trace, we drew the trace of the main geologic fault between nearby discontinuous ruptures by using major tectonic/geomorphologic features from available maps (inferred trace of the principal geologic fault in Fig.s S1, S2, S8, S9, S10 and S11).

Distributed ruptures were measured every 200 m along-strike the principal fault. In order to prevent that short ruptures would be missed or under-sampled during measurement, ruptures shorter than 200 m were measured at the midpoint, and ruptures between 200 and 400 m-long were measured at the midpoint and endpoints (Fig. 1). Moreover, all the points having displacement information on distributed ruptures were measured. All the points with displacement values on the principal fault rupture were also measured if distributed ruptures were associated with that strand of the principal fault. A particular metrics was used for the Sylmar segment of the San Fernando 1971 rupture zone (Fig. S1) where most of the distributed faulting was mapped along roads, resulting in a very discontinuous pattern of surface ruptures. In order to have a database of measurements statistically equivalent respect to the other studied earthquakes, variable measurement logics were used in order to sample ruptures at distances that equal more or less 200 m (see Fig. S1 for details).

All the distributed ruptures reported in the published maps as of primary (i.e., tectonic) origin were measured. Only the "Beni Rached" rupture zone of the 1981 El Asnam earthquake (Fig. S2) was not measured. It consists of normal fault ruptures interpreted to be related to either or both (Yelding et al., 1981; Philip and Meghraoui, 1983): 1) very large gravitational sliding; and 2) surface response of an unconstrained deep tectonic fault also responsible for the 1954 M 6.7 earthquake. Therefore, we avoided measuring the rupture due to the large uncertainties concerning its primary origin.

Some distributed ruptures reasonably unconnected with the main seismogenic fault were classified as sympathetic fault ruptures (Sy; Figs. S1, S2 and S5). We included in this category a rupture on a pre-existing thrust fault located more than 2 km in the hanging wall of the Chi-Chi 1999 principal fault rupture, due to its large distance from the main fault trace compared to all the other distributed ruptures (Tsauton East fault, Fig. S8), but a deep connection with the main seismogenic fault is possible (Ota et al., 2007a). The accuracy of the measurements depends on the scale of the original maps and on the level of detail reported in the maps. In this work only the detailed maps were considered, uncertain or inferred ruptures were not taken into account.

The measured ruptures have been classified according to the scarp types illustrated in Fig. 2, alternatively the scarp type was classified as "Unknown". Scarp types from "a" to "g" (Fig. 2) follow the scheme proposed by Philip et al. (1992), integrated with the classification of Yu et al. (2010). Concerning the scarp type, thrust earthquakes are characterized by a high variability of coseismic scarps due to the complex interaction between faulting and folding, geometry of the faults, and topography and rheology of the surface materials. The coseismic scarps can be classified according to the scheme first proposed by Philip et al. (1992) after the 1988 Spitak (Armenia) earthquake, integrated with the classification of Yu et al. (2010), which includes seven main types of thrust-related fault scarps and related secondary structures (Fig. 2). In case of steeply dipping faults, a simple thrust scarp in bedrock (type a) or a hanging wall collapse scarp in bedrock or in brittle unconsolidated material (type b) are produced. In case of low-angle faults and presence of soft-sediment covers, a number of various types of pressure ridges (types c to f) can be observed, depending on the displacement, sense of slip and behaviour of near-surface materials. In presence of shallow blind faults, a fault-related fold scarp may be formed (type g). Moreover, in this study also two additional types of thrust scarps structural contexts were distinguished, which are characterized by the occurrence of bending-moment and flexural-slip secondary fault ruptures (Yeats, 1986), associated with large-scale folds (hundreds of meters to kilometres in wavelength). Both of them these occurred widely during the 1980 El Asnam earthquake (Philip and Meghraoui 1983). Bending-moment faults (type h in Fig. 2) are normal faults that are formed close to the hinge zone of large-scale anticlines (extensional faults at the fold extrados in Philip and Meghraoui 1983), while flexural-slip faults (type i) are faults that are formed due to differential slip along bedding planes on the limbs of a bedrock fold (Yeats, 1986). Similar secondary Bending-moment distributed ruptures associated to with small-scale folds (meters to dozens of meters in wavelength), which form at the leading edge of the thrust, are not included in these two particular typesbelong to scarp types “c” to “g”. The measured rupture data has been classified according to the scarp types illustrated in Fig. 2 whenever possible; alternatively, the scarp type was classified as “Unknown”.

3 Width of the Rupture Zone (WRZ): statistical analysis

The most impressive and recurrent measured features are ruptures occurring along pre-existing fault traces and on the hanging wall, as the result of the reactivation of the main thrust at depth. Secondary structuresDistributed ruptures are mainly represented by synthetic and antithetic faults, which are parallel to or branching from the main fault. Fault segmentation and en échelon geometries are common in transfer zones or in oblique-slip earthquakes. The collected data was analysed in order to evaluate the width of the rupture zone (WRZ), intended as the total width, measured perpendicularly to the main faultprincipal fault rupture, within which all the secondary distributed ruptures occur. Figure 3 shows frequency distribution histograms of the distance of distributed rupturessecondary ruptures from the main principal fault (r) for all the analysed earthquakes. Negative values refer to the footwall, while positive values refer to the hanging wall. In particular, in Fig. 3a we distinguished the scarps with bending-moment (B-M), or flexural-slip (F-S) or sympathetic (Sy) secondary fault ruptures from the other types; in Fig. 3b the scarps without B-M, or F-S or Sy secondary fault ruptures are distinguished by scarp types, and in Fig. 3c the scarps with B-M, or F-S or Sy secondary fault ruptures are distinguished by earthquake. In general, although the values span over a large interval (-750 2,150 m to in the footwall; 1,6103,100 m in the hanging wall), most of them occur in the proximity of the main principal fault and display an asymmetric distribution between hanging wall and footwall.
In Fig. 3b all the data (excluding scarps with B-M, and F-S and Sy faults) are distinguished by scarp type. Simple Pressure Ridges with narrow WRZ (in green) prevail. Larger WRZ characterizes back-thrust, low-angle and oblique pressure ridges, and the relative data, together with those associated to the other pressure ridges (oblique, back-thrust and low-angle), span over an interval that is larger than for simple thrust scarps (in blue). This im-

plies implying that the main thrust geometry, the local kinematics and the near-surface rheology have a significant control in strain partitioning with consequences on the WRZ, as expected.

The occurrence of B-M or F-S secondary fault ruptures is strictly related to the structural setting of the earthquake area. In particular, B-M faults, which are related to the presence of large-scale hanging wall anticlines, were clearly observed in the El Asnam 1980 (Philip and Meghraoui, 1983) and Kashmir 2005 (southern part of central segment; Kaneda et al., 2008; Sayab and Khan, 2010) earthquakes. A wide extensional zone (1.8 km-long in the E-W direction; 1.3 km-wide) formed on the eastern hanging wall side of the Sylmar segment of the San Fernando 1971 surface rupture. The interpretation of such an extensional zone is not straightforward. Nevertheless, the presence of a macro-anticline in the hanging wall of the Sylmar fault is indicated by subsurface data (Mission Hill anticline; Tsutsumi and Yeats, 1999). Though it is not possible to clearly classify these structures as B-M faults in strict sense, it seems reasonable to interpret them as generic fold-related secondary extensional faults. Therefore, they were plotted in Fig.s 3a and 3c together with B-M and F-S faults. F-S faults were observed on the upright limb of a footwall syncline in the El Asnam 1980 earthquake. As shown in Fig. 3a, the B-M and F-S datasets contribute significantly in widening the WRZ and are distributed only on the hanging wall or on the footwall of the main fault, respectively. Notably, the distribution of the B-M faults for the El Asnam earthquake is very similar to the distribution of extensional ruptures for the San Fernando earthquake (Fig. 3c). Ruptures close to the main fault (r < 200 150 m) are due to processes operating in all the other types of scarp types (Fig. 3b), but for larger distances (r > ~300 m) they the distributed faulting can be affected by other processes such as related to large-scale folding of a large-scale anticlineor sympathetic reactivation of pre-existing faults (Fig.s 3a and 3c), contributing significantly in widening the WRZ. with a larger frequency between 300 and 1,000 m from the main fault. The B-M ruptures for the Kashmir 2005 earthquake are localized in a narrower zone (≤ 200 m) closer to the main fault, due to the shorter wavelength of the hosting anticline.

In order to analyseFor the analysis of the statistical distribution of "r", the collected data was fitted with a number of probability density functions by using the commercial software EasyFitProfessional©V.5.6 (http://www.mathwave.com), which finds the probability distribution that best fits the data and automatically tests the goodness of the fitting. We decided to analyse both the database without B-M, F-S and Sy ruptures (called here "simple thrust" distributed ruptures; Fig. 4) and the entire database of distributed ruptures without filtering (Fig. 5). The aim is to analyse separately: 1) distributed ruptures that can be reasonably related only to (or preferentially to) the coseismic propagation to the ground surface of the main fault rupture; they are expected to occur in a rather systematic way compared to the main fault trace; and 2) distributed ruptures that are affected also by other, non-systematic structural features, mostly related to large-scale coseismic folding. Considering that

Commento [UW4]: Comment 3 of Rev. 1
Comment 1 of Rev. 2

the width of the rupture zone for the scarps with B-M and F-S is strictly related to the structural setting of the area (presence and wavelength of the fold), in this study only the scarp types without B-M and F-S (called here “simple thrust ruptures”) were analysed. The aim is to find a criterion for removing the outliers and sizing the zones within which surface fault ruptures are expected to occur. The hanging wall and footwall data was were fitted separately and the results are synthesized in Fig.s 4 and 5, where the best fitting distribution curves and the cumulative curves, selected by the software according to the Kolmogorov-Smirnov test, are shown. The same continuous function was found for both the hanging wall and footwall, which is the Birnbaum-Saunders (Fatigue Life) distribution.

For “simple thrust” distributed ruptures, The the hanging wall data (Figs. 4a and 4b) has a modal value of 5.57.1 m. The 90% probability (0.9 of the cumulative distribution function, HW90) seems to be a reasonable value to cut off the outliers (flat part of the curves). It corresponds to a distance of ~320 575 m from the main principal fault. From a visual inspection of the The histogram (Fig. 4b), there is an evident sharp drop of the data approximately at the 35% probability (HW35), corresponding to a distance of ~40 m from the principal fault. shows a zone close to the main fault, bounded by the 40% probability, where most of the ruptures occur (HW40, corresponding to ~30 m from the main fault). A The second sharp drop of the data in the histogram occurs at close to the 50% probability (HW50, corresponding to ~45 80 m from the main principal fault). Also the 3rd quartile is shown (HW75), corresponding to a distance of ~140 260 m from the main fault. The widths of the zones for the different probabilities (90%, 75%, 50% and 4035%) are listed in Table 2a.

The footwall data (Figs. 4c and 4d) has a modal value of the best fitting probability density function of 4 5 m. By applying the same percentiles used for the hanging wall, a 90% cut off (FW90) was found at a distance of ~145 265 m from the main principal fault. The FW75, FW50 and FW40 FW35 correspond to distances of ~70 120 m, ~25 45 m and ~20 m from the main principal fault, respectively (Table 2a). It is worth noticing that also for the footwall the 4035% probability corresponds to a sharp drop of the data.bounds reasonably well the zone where the most of the ruptures occur.

The ratio between the width of the rupture zone on the footwall and the width of the rupture zone on the hanging wall ranges from 1:1.5 8 to 1:2.2 (Table 2a), and therefore it is always close to 1:2 independently from the used percentile.

The results of the analysis performed on the entire database of distributed ruptures, including also the more complex secondary structures of B-M, F-S and Sy ruptures, is illustrated in Fig. 5 and summarized in Table 2b. As expected, the WRZ is significantly larger than for “simple thrust” distributed ruptures. The HW90, HW75 and HW50 correspond to distances of ~1100 m, ~640 m and ~260 m from the principal fault, respectively. For com-

Commento [UW5]: Comment 3 of Rev. 1
Comment 1 of Rev. 2

parison with the “simple thrust” distributed ruptures, also the HW35 was calculated (~130 m), but it does not correspond with a particular drop of the data in the histogram of Fig. 5b. Instead, a sharp drop is visible at a distance of ~40 m from the principal fault, as for the “simple thrust” database. In the footwall, the FW90, FW75 and FW50 correspond to distances of ~720 m, ~330 m and ~125 m from the principal fault, respectively. The FW35 corresponds to a distance of ~65 m, but the sharp drop of the data in the histogram of Fig, 5d is at a distance of ~20 m from the principal fault, as for the “simple thrust” database.

In order to analyse the potential relationships between WRZ and the earthquake size, in Fig. 5 6 the total width of the rupture zone (WRZ tot = WRZ hanging wall + WRZ footwall) is plotted against the Mw (Fig. 6a) and, for the subset of data having displacement information, against the vertical displacement (VD) on the principal fault (Fig. 6b).displacement on the main fault (vertical component, VD) for the subset of data having displacement information. The vertical displacement measured at the ground surface is highly sensitive to the shallow geometry of the thrust plane. The net displacement along the slip vector is a more appropriate parameter for considering the size of the displacement at the surface. However, the net displacement is rarely given in the literature, or can be obtained only by assuming a fault dip, while VD is the most commonly measured parameter. Therefore, we used VD as a proxy of the amount of surface displacement. In Fig. 6a a positive relation between the total WRZ and Mw is clear, particularly if sympathetic (Sy) fault ruptures are not considered. In fact, Sy data appear detached from the other data, suggesting that their occurrence is only partially dependent on the magnitude of the mainshock. They also depend on the structural features of the area, such as 1) whether or not an active, favourably-oriented fault is present, and 2) its distance from the main seismogenic source. Though a broad positiveA correlation between the total WRZ and VD can be speculated, especially if the data with B-M and F-S faults is excluded, a clear correlation is not obvious (Fig. 5a6b). Even for small values of VD (< 1 m) the total WRZ can be as wide as hundreds of meters, but a larger number of displacement data is necessary for drawing convincing conclusions. A possible correlation can be found by zooming in the diagram in the area close to the main fault (WRZ <200 m, Fig. 5b). Close to the main fault (WRZ < 60 m), the width of the rupture zone appears to have a nearly linear upper boundary which correlates positively with VD, for VD < ~2 m (dashed line in Fig. 5b). This suggests that close to the main fault the width of the rupture zone increases with displacement, from a minimum of nearly 20 m for decimetric VD up to 50-60 m for VD close to 2 m. However, also for VD <2 m, the maximum WRZ, including the secondary ruptures away from the main fault, can be up to 200 m or wider.

4 Comparison with Italian guidelines and implications for fault zoning during seismic microzonation

The definition of the WRZ based on the analysis of the data from worldwide thrust earthquakes can support the evaluation and mitigation of SFRH. The values reported in Table 2 can be used for shaping and sizing fault zones (e.g. Warning or Susceptible Zones in the Italian guidelines; Earthquake Fault Zones in the A-P Act) and avoidance zones around the trace of active thrust faults (Table 3).

A first question that needs to be answered is which set of data between “simple thrust” distributed ruptures (Fig. 4; Table 2a) and all distributed ruptures (Fig. 5, Table 2b) is the most appropriate to be used for sizing the fault zones. The answer is not easy and implicates some subjective choices. In Table 3 we suggest using the results from “simple thrust” distributed ruptures. The results from all distributed ruptures can be used in areas with poor geologic knowledge, in order to assess the extent of the area within which potential sources of fault displacement hazard can be present. Our choices result from the following line of reasoning:

Commento [UW6]: Comment 3 of Rev. 1
Comment 1 of Rev. 2

1) The data analysed in this work are from brittle rupture of the ground surface. The measured distributed ruptures are always associated with surface faulting on the principal fault. Therefore, the results can be used for zoning the hazard deriving from mechanisms connected with the propagation of the rupture on the main fault plane up to the surface. Deformations associated with blind thrusting are not analysed. Therefore, the results are not suitable for zoning ductile tectonic deformations associated with blind thrusting (e.g. folding). Clearly, coseismic folding occurs both during blind thrusting and surface faulting thrusting. Furthermore, brittle surface ruptures and other ductile deformations can be strictly connected to each other, making difficult to separate the two components, but a global analysis of the entire spectrum of permanent tectonic deformation associated to thrust faulting need additional data not considered here.

2) In most cases, distributed ruptures occur on secondary structures that are small and cannot be recognized before the earthquake, or that only site-specific investigations could distinguish. Fault zones should include the hazard from this kind of ruptures.

3) Some secondary faults connected with the principal fault can be sufficiently large to have their own geologic and geomorphic signature, and can be recognized before the earthquake. Most likely, close to the surface these structures behave similarly to the principal fault, with their own distributed ruptures. Faults with these characteristics should have their own zone, unless they are included in the principal fault zone.

4) Point 3 also applies to distant large active faults that can undergo sympathetic triggering. They should be zoned as separate principal faults. Using Sy ruptures for shaping zones of fault rupture hazard would imply distributing the hazard within areas that can be very large (Fig.s 5, 6). The size of the resulting zone would depend

mostly on the structural setting of the analysed areas (presence or not of the fault, distance from the seismogenic source) rather than the mechanics which controls distributed faulting in response to principal faulting.

5) B-M and F-S fault ruptures are not always present. Where present, they occur over distances ranging from hundreds of meters to kilometers (Fig. 3c). In any case, B-M and F-S secondary faults are strictly related to the structural setting of the area (large-scale folding; fold shape, wavelength and tightness; stiffness of folded strata). In fact, B-M fault ruptures commonly observed in historical earthquakes are normal faults. B-M normal faults are expected to occur in the shallowest convex (lengthened) layer of the folded anticline. They can occur only where the bending stress is tensional, that is the convex side of the folded layer, preferentially close to the crest of the anticline and parallel to the anticline hinge. F-S faults can rupture the surface where the steeply-dipping limb of a fold is formed by strata of stiff rocks able to slip along bedding planes (e.g. Fig. 2i). Moreover, it is known that coseismic B-M or F-S faults often reactivate pre-existing fault scarps (e.g. Yeats, 1986) which might help in zoning the associated potential fault rupture hazard before the earthquake. Therefore, knowledge of the structural setting of the area can help in identifying zones potentially susceptible to B-M or F-S faulting, which should be zoned as separate sources of fault rupture hazard.

In Table 3, the total WRZ from the present study is compared with the sizes of the zones proposed by the Italian guidelines for SM studies (Technical Commission for Seismic Microzonation, 2015; SM Working Group, 2015). The values reported in Table 3 ~~table~~ ~~can~~ could be used~~considered as a proposal~~ for integrating the existing criteria. In particular, the total WRZ from "simple thrust" distributed ruptures is used for sizing Warning Zones (Level 1 SM) and Susceptible and Avoidance Zones (Level 3 SM). The total WRZ from all distributed ruptures is suggested to be used for sizing Warning Zones in areas with poor basic geologic knowledge (Level 1 SM).

Commento [UW7]: Comment 4 of Rev. 1

The first observation is that the FW:HW ratio proposed by the Italian guidelines is supported by the results of this study (FW:HW ratio close to 1:2).

Assuming that the 90% probability is a reasonable criterion for cutting the outliers from the analysed population, the resulting total WRZ (HW + FW) for "simple thrust" distributed ruptures is ~~465~~ 840 m (560 m on the HW + 280 m on the FW). This width could be used for zoning all the reasonably inferred fault rupture hazard, from both the ~~main~~ principal fault and ~~secondary~~ distributed ~~faults~~ruptures, during basic (Level 1) SM studies, which do not require high-level specific investigations. The obtained value is ~~not very~~significantly different from that recommended by the Italian guidelines for Level 1 SM (400 m).

~~The most~~A significant ~~evident~~ difference between our proposal and the Italian guidelines concerns also the width of the zone that should be avoided, due to the very high likelihood of having surface ruptures. Though the entire rupture zone could be hundreds of meters wide, ~~40-50% of~~more than one third of ~~secondary~~ distributed ruptures are expected to occur within a narrow, ~~50-7~~60 ~~m~~ m-wide zone. As could be expected, only site-specific paleo-sismologic investigations can quantify the hazard from surface faulting at a specific site. In the absence of such a detail, and for larger areas (e.g. municipality scale) the fault avoidance zone should be in the order of ~~50-7~~60 m, shaped asymmetrically compared to the trace of the main fault (~~30-45~~40 m on the HW; 20~~-25~~ m on the FW). ~~Figure 5b suggests a positive relation between the displacement on the main fault and the width of the rupture zone close to the main fault (WRZ ≤ 60 m). Assuming that this relation is real, Fig. 5b suggests that the avoidance zone should be larger than 20-30 m, even for displacements of a few decimetres.~~

In Table 3 a width of ~~210~~ 380 m is proposed for the susceptible zone (Level 3 SM). The choice of defining the width of the zone as the 3rd quartile (3 out of 4 probability that secondary faulting lies within the zone) is rather arbitrary. In fact, the width of the susceptible zone should be flexible. Susceptible zones are used only if uncertainties remain also after high-level seismic microzonation studies, such as uncertainties on the location of the main fault trace or about the possibility of secondary faulting away from the main fault. Susceptible zones can also be used for areas where a not better quantifiable distributed faulting might occur, such as in structurally complex zones (e.g. stepovers between main fault strands).

~~It is important to underline that the proposed criteria are applicable only to simple thrust ruptures, without B-M or F-S faults. B-M and F-S secondary faults are strictly related to the structural setting of the area (large-scale folding). Therefore, knowledge of the structural setting of the area may help in identifying zones potentially susceptible to B-M or F-S faulting. In fact, the B-M surface-ruptures commonly observed in historical earthquakes are normal faults. B-M normal faults are expected to occur in the shallowest convex (lengthened) layer of the folded anticline. They can occur only where the bending stress is tensional, that is the convex side of the folded layer, preferentially close to the crest of the anticline and parallel to the anticline hinge. F-S faults can rupture the surface where steeply-dipping limbs of folds associated to the seismogenic thrust, formed by stiff strata able to slip along bedding planes, intersect the topography (e.g. Fig. 2i). Thus, zones of potential B-M or F-S secondary faulting can be traced by knowing the geometry and wavelength of the fold and the first order stiffness of the folded material. Moreover, it is known that coseismic B-M or F-S faults often reactivate pre-existing fault scarps (e.g. Yeats, 1986) being the geomorphic signature which might help in zoning the associated SFRH.~~

5 Conclusions

The distribution of coseismic surface ruptures (distance of distributedsecondary ruptures from the main principal fault rupture) for 10 11 well-documented historical surface faulting thrust earthquakes (5.4 ≤ M ≤ 7.9) provide constraints on the general characteristics of the surface rupture zone, with implications for zoning the surface rupture hazard along active thrust faults.

Secondary Distributed ruptures can occur up to large distances from the main principal fault (~750 m on the footwall and ~1,600 m up to ~3,000 m on the hanging wall), but most of them occur within few dozens of meters from the main principal fault. The distribution of secondary ruptures is asymmetric, with most of them located on the hanging wall. Coseismic folding of large-scale folds (hundreds of meters to kilometres in wavelength) may produce bending-moment (B-M) or flexural-slip (F-S) secondary fault ruptures on the hanging wall and footwall, respectively, widening significantly the rupture zone. Additional widening of the rupture zone can be due to sympathetic slip on distant active faults (Sy fault ruptures).

The distribution of secondary ruptures for "simple thrust" ruptures (without B-M, and F-S, and Sy fault ruptures) can be fitted by a continuous probability density function, of the same form for both the hanging wall and footwall. This function can be used for removing outliers from the analyzed analysed database (e.g. 90% probability) and define cold criteria for shaping SFRH zones. These zones can be used during seismic microzonation studies and can help in integrating existing guidelines.

The 90% probability of the cumulative distribution function defines a rupture zone of ~320 m-wide on the hanging wall and ~145 m-wide on the footwall (total width of ~465 m). This wide zone could be used for zoning SFRH during basic seismic microzonation studies (i.e. Level 1 SM according to the Italian guidelines), which typically lack of specific investigations and therefore are characterized by uncertainties on the location of the main fault and on the occurrence of secondary faulting away from the main fault.

More than 40-50%one third of the ruptures are expected to occur within a zone of ~60 30-45 m-wide on the hanging wall and 20-25 m-wide on the footwall (total width being 50-70 m). This narrow zone could be used for defining the fault avoiding zone during high-level, municipality-scale seismic microzonation studies (i.e. Level 3 SM according to the Italian guidelines). The average FW:HW ratio of the WRZ -is close to 1:2, independently from the used percentile.

A possible positive relation between the displacement on the main fault and the total width of the rupture zone (total WRZ) is found only close to the main fault (total WRZ ≤ 60 m). Close to the main fault, the WRZ appears to increase with displacement, from a minimum of nearly 20-30 m for decimetric vertical displacement (VD) up to 50-60 m for VD close to 2 m. This suggests that the avoidance zone should be larger than 20-30 m, even for displacements of a few decimetres.

The average FW:HW ratio of the WRZ is close to 1:2, independently from the used percentile.

In addition to the expected rupture zone along the trace of the main thrust, zones potentially susceptible to B-M or F-S secondary faulting can be inferred identified by detailed knowledge of the structural study setting of the area (shape, wavelength, tightnessgeometry, wavelength and lithology of the thrust-related large-scale folds) and by scrutinize possible geomorphic traces of past secondary faulting. Where recognized, these areas should have their own zones of fault rupture hazard.

The analysis of the entire database of distributed ruptures (Fig. 5) indicates significantly larger rupture zones compared to the database without B-M, F-S and Sy ruptures. This is due to the combination of processes related to the propagation up to the surface of the main fault rupture and other processes associated with large-scale co-seismic folding, as well as triggering of distant faults. These data can be useful in poorly-known areas, in order to assess the extent of the area within which potential sources of fault displacement hazard can be present.

The results from this study, particularly the function obtained in Fig. 4, can be used for improving the attenuation relationships for distributed faulting with distance from the principal fault, with possible applications in probabilistic studies of fault displacement hazard (e.g., Youngs et al., 2003; Petersen et al., 2011).

Commento [UW8]: Comment 3 of Rev. 2

Competing interests

The authors declare that they have no conflict of interest.

Acknowledgements

The project was funded by Department DiSPUTer, "G. D'Annunzio" University of Chieti-Pescara (research funds to P. Boncio).

References

Commento [UW9]: References have been updated

Angelier, J., Lee, J. C., Chu, H. T., and Hu, J. C.: Reconstruction of fault slip of the September 21st, 1999, Taiwan earthquake in the asphalted surface of a car park, and co-seismic slip partitioning, J. Struct. Geol., 25, 345-350, 2003.

Avouac, J. P., Ayoub, F., Leprince, S., Konea, O., and Helmberger, V.: The 2006 Mw 7.6 Kashmir earthquake: sub-pixel correlation of ASTER images and seismic waveforms analysis, Earth Planet. Sci. Lett., 249, 514-528, 2006.

Bilham, R. and Yu, T. T.: The morphology of thrust faulting in the 21 September 1999, Chichi, Taiwan earthquake, J. Asian Earth Sci., 18, 351-367, 2000.

Boncio, P., Galli, P., Naso, G., and Pizzi, A.: Zoning Surface Rupture Hazard along Normal Faults: Insight from the 2009 M_W 6.3 L'Aquila, Central Italy, Earthquake and Other Global Earthquakes, Bull. Seism. Soc. Am., 102, 918-935, doi: 10.1785/0120100301, 2012.

Bowman, J. R. and Barlow, B. C.: Surveys of the fault scarp of the 1986 Marryat Creek, South Australia, earthquake, [Australian] Bureau of Mineral Resources, Geology and Geophysics Record 1991/190, 12 pp., 3 plates, 1991.

Bryant, W. A. and Hart, E. W.: Fault-Rupture Hazard Zones in California, Alquist-Priolo Earthquake Fault Zoning Act With Index to Earthquake Fault Zones Maps, Calif Geol. Surv. Spec. Pub., 42, 41 pp, 2007.

Central Geological Survey, MOEA at http://gis.moeacgs.gov.tw/gwh/gsb97-1/sys8/index.cfm

Chang, J. C. and Yang, G. S.: Deformation and occurrence of the Che-lung-pu Fault from geomorphic evidence, Quat. Int., 115-116, 177-188, 2004.

Chen, C. H., Chou, H.S., Yang, C.Y., Shieh, B. J., and Kao, Y. H.: Chelungpu fault inflicted damages of pile foundations on FWY rout 3 and Fault zoning regulations in Taiwan, A Workshop on Seismic Fault-induced Failures, Tokyo, 2003.

Chen, G. H., Xu, X. W., Zheng, R. Z., Yu, G. H., Li, F., Li, C. X., Wen, X. Z., He, Y. L., Ye, Y. Q., Chen, X. C., and Wang, Z. C.: Quantitative analysis of the co-seismic surface rupture of the 2008 Wenchuan earthquake, Sichuan, China along the Beichuan-Yingxiu Fault, Seismol. Geol., 30 (3), 723-738, 2008 (in Chinese with English abstract).

Chen, W. C., Chu, H. T., and Lai, T. C.: Surface ruptures of the Chi-Chi Earthquake in the Shihgang Dam area, Special Issue for the Chi-Chi Earthquake, 1999, Special Publication of the Central Geological Survey, 12, 41-62, 2000 (in Chinese with English abstract).

Crone, A. J., Machette, M. N., and Bowman, J. R.: Geologic investigations of the 1988 Tennant Creek, Australia, earthquakes— Implications for paleoseismicity in stable continental regions, U.S. Geol. Surv. Bull. 2032-A, A1–A51, 1992.

Dong S, Zhang Y, Wu Z, Yang, N., Ma, Y., Shi, W., Chen, Z., Long, C., and An, M.: Surface Rupture and Co-seismic Displacement Produced by the Ms8.0 Wenchuan Earthquake of May 12th, 2008, Sichuan, China: Eastwards Growth of the Qinghai-Tibet Plateau, Acta Geol. Sin., 82 (5), 938-948, 2008a.

Dong, S., Han, Z., and An, Y.: Surface deformation at the epicenter of the May 12, 2008 Wenchuan M8 Earthquake, at Yingxiu Town of Sichuan Province, China, Sci. China Ser. E, 51, 154–163, doi:10.1007/s11431-008-6007-0, 2008b.

Faccioli, E., Anastasopoulos, I., Gazetas, G., Callerio, A., and Paolucci R.: Fault rupture–foundation interaction: selected case histories, Bull. Earthquake Eng., 6 (4), 557-583, 2008.

Fredrich, J., McCaffrey, R., and Denham, D.: Source parameters of seven large Australian earthquakes determined by body waveform inversion, Geoph. J., 95, 1-13, 1988.

Haessler, H., Deschamps, A., Dufumier, H., Fuenzalida, H. and Cisternas, A.: The rupture process of the Armenian earthquake from broad-band teleseismic body wave records, Geophys. J. lnt., 109, 151-161, 1992.

Huang, C., Chan, Y. C., Hu, J. C., Angelier, J., and Lee, J. C.: Detailed surface co-seismic displacement of the 1999 Chi-Chi earthquake in western Taiwan and implication of fault geometry in the shallow subsurface, J. Struct. Geol., 30, 1167-1176, 2008.

Huang, W. J., Chen, Z. Y., Liu, S. Y., Lin, Y. H., Lin, C. W., and Chang, H. C.: Surface deformation models of the 1999 Chi–Chi earthquake between Tachiachi and Toupienkengchi, central Taiwan, Special Issue for the Chi-Chi Earthquake, 1999, Special Publication of the Central Geological Survey, 12, 63–87, 2000 (in Chinese with English abstract).

Huang, W. J.: Deformation at the leading edge of thrust faults, Ph.D. dissertation, Purdue University, West Lafayette, Indiana, 435 pp., 2006.

Ishimura, D., Okada, S., Niwa, Y., and Toda, S.: The surface rupture of the 22 November 2014 Nagano-ken-hokubu earthquake (Mw 6.2), along the Kamishiro fault, Japan, Active Fault Research, 43, 95-108, 2015 (in Japanese with English abstract).

Kaneda, H., Nakata, T., Tsutsumi, H., Kondo, H., Sugito, N., Awata, Y., Akhtar, S. S., Majid, A., Khattak, W., Awan, A. A., Yeats, R. S., Hussain, A., Ashraf, M., Wesnousky, S. G. and Kausar, A. B.: Surface rupture of the 2005 Kashmir, Pakistan, Earthquake and its active tectonic implications, Bull. Seismol. Soc. Am., 98, 521–557, 2008.

Kawashima, K.: Damage of bridges resulting from fault rupture in the 1999 Kocaeli and Dunce, Turkey earthquakes and the 1999 Chi-Chi, Taiwan earthquake, Structural Engineering/Earthquake Engineering, 19(2), 179s–197s, 2002.

Kelson, K. I., Kang, K. H., Page, W. D., Lee, C. T., and Cluff, L. S., 2001: Representative styles of deformation along the Chelungpu Fault from the 1999 Chi-Chi (Taiwan) earthquake: geomorphic characteristic and responses of man-made structures, Bull. Seismol. Soc. Am., 91(5), 930–952, 2001.

Kelson, K. I., Koehler, R. D., Kang, K.-H., Bray, J. D. and Cluff, L. S.: Surface deformation produced by the 1999 Chi-chi (Taiwan) earthquake and interactions with built structures, Final Technical Report, U.S.G.S. Award No. 01-HQ-GR-0122, 21 pp., 2003.

Kerr, J., Nathan, S., Van Dissen, R., Webb, P., Brunsdon, D., and King, A.: Planning for development of land on or close to active faults: A guide to assist resource management planners in New Zealand. Report prepared for the Ministry for the Environment by the Institute of Geological & Nuclear Sciences, Client Report 2002/124, Project Number 440W3301, 2003.

Konagai, K., Hori, M., Meguro, K., Koseki, J., Matsushima, T., Johansson, J., and Murata, O.: Key Points for Rational Design for Civil Infrastructures near Seismic Faults Reflecting Soil-Structure Interaction Features, Report of JSPS research project, grant-in-aid for scientific research (A) Project No.16208048, 2006.

Kumahara, Y. and Nakata, T.: Recognition of active faults generating the 2005 Pakistan earthquake based on interpretation of the CORONA satellite photographs, E-journal GEO, 2 (2), 72-85, 2007 (In Japanese with English abstract).

Lee, G. C. and Loh, C. H. (Eds): The Chi-Chi, Taiwan Earthquake of September 21, 1999: Reconnaissance Report, Technical Report MCEER-00-0003 April 30, 2000.

Lee, J. C. and Chan, Y. C.: Structure of the 1999 Chi-Chi earthquake rupture and interaction of thrust faults in the active fold belt of western Taiwan, J. Asian Earth Sci., 31, 226-239, 2007.

Lee, J. C., Chen, Y. G., Sieh, K., Mueller, K., Chen, W. S., Chu, H. T., Chan, Y. C., Rubin, C., and Yeats, R.: A Vertical Exposure of the 1999 Surface Rupture of the Chelungpu Fault at Wufeng, Western Taiwan: Structural and Paleoseismic Implications for an Active Thrust Fault, Bull. Seismol. Soc. Am., 91, 5, pp. 914-929, 2001.

Lee, Y. H., Hsieh, M. L., Lu, S. D., Shih, T. S., Wu, W. Y., Sugiyama, Y., Azuma, T., and Kariya, Y.: Slip vectors of the surface rupture of the 1999 Chi-Chi earthquake, western Taiwan, J. Struct. Geol., 25, 1917-1931, 2003.

Lee, Y. H., Wu, K. C., Rau, R. J., Chen, H. C., Lo, W., and Cheng, K. C.: Revealing coseismic displacements and the deformation zones of the 1999 Chi-Chi earthquake in the Tsaotung area, central Taiwan, using digital cadastral data, J. Geophys. Res., 115, B03419, 2010.

Lettis, W. R., Wells, D. L., and Baldwin, J. N.: Empirical observations regarding reverse earthquakes, blind thrust faults, and quaternary deformation: Are blind thrust faults truly blind?, Bull. Seismol. Soc. Am., 87(5), 1171–1198, 1997.

Lin, A., Sano, M., Yan, B., and Wang, M.: Co-seismic surface ruptures produced by the 2014 Mw 6.2 Nagano earthquake, along the Itoigawa–Shizuoka tectonic line, central Japan, Tectonophysics, 656, 142-153, 2015.

Lin, W. H.: On surface deformations from the Chi-Chi earthquake in the Shihkang and Chutzekeng areas, Special Issue for the Chi-Chi Earthquake, 1999, Special Publication of the Central Geological Survey, 12, 1-17, 2000 (in Chinese with English abstract).

Liu-Zeng, J., Sun, J., Wang, P., Hudnut, K. W., Ji, C., Zhang, Z., Xu, Q., and Wen, L.: Surface ruptures on the transverse Xiaoyudong fault: A significant segment boundary breached during the 2008 Wenchuan earthquake, China, Tectonophysics 580, 218–241, 2012.

Liu-Zeng, J., Sun, J., Zhang, Z., Wen, L., Xing, X., Hu, G., and Xu, Q.: Detailed mapping of surface rupture of the Wenchuan Ms 8.0 earthquake near Hongkou and seismotectonic implications, Quaternary Sciences, 30 (1), 1-29, 2010 (in Chinese with English abstract).

Liu-Zeng, J., Zhang, Z., Wen, L., Tapponnier, P., Sun, J., Xing, X., Hu, G., Xu, Q., L. Zeng, L., Ding, L., Ji, C., Hudnut, K.W., and van der Woerd, J.: Co-seismic ruptures of the 12 May 2008, Ms 8.0 Wenchuan earthquake, Sichuan: East–west crustal shortening on oblique, parallel thrusts along the eastern edge of Tibet, Earth Plan. Sci. Lett., 286, 355-370, 2009.

Machette, M. N., Crone, A. J., and Bowman, J. R.: Geologic investigations of the 1986 Marryat Creek, Australia, earthquakes - implications for paleoseismicity in stable continental regions, U.S. Geol. Sur. Bull. 2032-B, 29, 1993.

McCaffrey, R.: Teleseismic investigation of the January 22, 1988 Tennant Creek, Australia, earthquakes, Geophys. Res. Lett., 16, 413-416, 1989.

Meghraoui, M., Jaegy, R., Lammali, K., and Albarède, F.: Late Holocene earthquake sequences on the El Asnam (Algeria) thrust fault, Earth Planet. Sci. Lett., 90, 187–203, 1988.

Okada, S., Ishimura, D., Niwa, Y., and Toda, S.: The First Surface-Rupturing Earthquake in 20 Years on a HERP Active Fault is Not Characteristic: The 2014 Mw 6.2 Nagano Event along the Northern Itoigawa–Shizuoka Tectonic Line, Seismol. Res. Lett., 86 (5), 1–14, 2015.

Ota, Y., Huang, C. Y., Yuan, P. B., Sugiyama, Y., Lee, Y. H., Watanabe, M., Sawa, H., Yanagida, M., Sasaki, S., Suzuki, Y., Tang, H. S., Shu, U.T., Yang, S. Y., Hirouchi, D., and Taniguchi, K.: Trenching Study at the

Tsautun Site on the Central Part of The Chelungpu Fault, Taiwan, J. Geogr., 110 (5), 698-707, 2001 (in Japanese with English abstract).

Ota, Y., Shishikura, M., Ichikawa, K., Watanabe, M., Yanagida, M., Tanaka, T., Sawa, H., Yamaguchi, M., Lee, Y. H., Lu, S. T., Shih, T. S., and Amagasa, S.: Low-angle reverse faulting during two earthquakes on the northern part of the Chelungpu fault, deduced from the Fengyuan trench, Central Taiwan, Terr. Atmos. Ocean. Sci., v. 18, no. 1, p. 55–66, 2007b.

Ota, Y., Watanabe, M., Suzuki, Y., Yanagida, M., Miyawaki, A., and Sawa, H.: Style of the surface deformation by the 1999 Chichi earthquake at the central segment of Chelungpu fault, Taiwan, with special reference to the presence of the main and subsidiary faults and their progressive deformation in the Tsauton area, J. Asian Earth Sci., 31, 214-225, 2007a.

Petersen, M., Dawson, T.E., Chen, R., Cao, T., Wills, C.J.,Schwartz, D.P., and Frankel, A.D.: Fault displacement hazard for strike-slip faults, Bull. Seismol. Soc. Am, 101 (2), 805–825, 2011.

Philip, H. and Meghraoui, M.: Structural analysis and interpretation of the surface deformation of the El Asnam earthquake of October 10, 1980, Tectonics, 2, 17-49, 1983.

Philip, H., Rogozhin, E., Cisternas, A., Bousquet, J. C., Borisov, B., and Karakhanian, A.: The Armenian earthquake of 1988 December 7: faulting and folding, neotectonics and palaeoseismicity, Geophys. J. Int., 110, 141-158, 1992.

Rajendran, C. P., Rajendran, K., Unnikrishnan, K. R., and John, B.: Palaeoseismic indicators in the rupture zone of the 1993 Killari (Latur) earthquake, Curr. Sci., 70 (5), 385-390, 1996.

Rymer, M. J., Kendrick, K. J., Lienkaemper, J. J., and Clark, M. M.: Surface rupture on the Nunez fault during the Coalinga earthquake sequence, in Rymer, M.J, and Ellsworth, W.L. eds., The Coalinga, California, Earthquake of May 2, 1983, U.S. Geol. Sur. Prof. Paper 1487, 299-318, 1990.

Sayab, M. and Khan, M.A.: Temporal evolution of surface rupture deduced from coseismic multi-mode secondary fractures: Insights from the October 8, 2005 (Mw 7.6) Kashmir earthquake, NW Himalaya, Tectonophysics, 493, 58–73, 2010.

Seeber, L., Ekstrom, G., Jain, S.K., Murty, C.V.R., Chandak, N., and Armbruster, J. G.: The 1993 Killari earthquake in central India: a new fault in Mesozoic basalt flows?, J. Geophys. Res., 101, 8543-8560, 1996.

Shin, T. C. and Teng, T. L.: An overview of the 1999 Chi-Chi, Taiwan, Earthquake, Article in Bull. Seismol. Soc. Am., 91(5), 895-913, 2001

SM Working Group: Guidelines for Seismic Microzonation, Conference of Regions and Autonomous Provinces of Italy, Civil Protection Department, English edition of: Gruppo di lavoro MS, Indirizzi e criteri per la microzonazione sismica, Conferenza delle Regioni e delle Province autonome – Dipartimento della protezione civile, Roma, 2008, 3 vol. e Dvd, 2015. Available online at http://www.protezionecivile.gov.it/httpdocs/cms/attach_extra/GuidelinesForSeismicMicrozonation.pdf, 2015.

Technical Commission for Seismic Microzonation: Linee guida per la gestione del territorio in aree interessate da Faglie Attive e Capaci (FAC), versione 1.0, Conferenza delle Regioni e delle Province Autonome – Dipartimento della Protezione Civile, 55 pp., Roma, 2015 (In Italian).

Tsutsumi, H. and Yeats, R.: Tectonic setting of the 1971 Sylmar and 1994 Northridge earthquakes in the San Fernando valley, California, Bull. Seism. Soc Am., 89 (5), 1232-1249, 1999.

U.S. Geological Survey Staff: Surface faulting, in: The San Fernando, California, earthquake of February 9, 1971, U.S. Geol. Sur. Prof. Paper 733, 55-76, 1971.

Wang, H., Ran, Y, Chen, L., Shi, X., Liu, R., and Gomez, F.:Determination of horizontal shortening and amount of reverse-faulting from trenching across the surface rupture of the 2008 Mw 7.9 Wenchuan earthquake, China, Tectonophysics, 491, 10–20, 2010.

Wells, D. and Coppersmith, K.: New empirical relationships among magnitude, rupture length, rupture width, rupture area, and surface displacement, Bull. Seismol. Soc. Am., 84 (4), 974-1002, 1994.

Wesnousky, S. G.: Displacement and geometrical characteristics of earthquake surface ruptures: Issues and implications for seismic hazard analysis and the earthquake rupture process, Bull. Seismol. Soc. Am., 98(4), 1609–1632, 2008.

Xu, X., Wen, X., Ye, J., Ma, B., Chen, J., Zhou, R., He, H., Tian, Q., He, Y., Wang, Z., Sun, Z., Feng, X., Yu, G., Chen, L., Chen, G., Yu, S., Ran, Y., Li, X., Li, C., and An, Y.: The Ms 8.0 Wenchuan earthquake surface ruptures and its seismogenic structure, Seismol. Geol., 30 (3), 597-629, 2008 (in Chinese with English abstract).

Xu, X., Wen, X., Yu, G., Chen, G., Klinger, Y., Hubbard, J., and Shaw, J.: Co-seismic reverse- and oblique-slip surface faulting generated by the 2008 Mw 7.9 Wenchuan earthquake, China, Geology 37(6), 515–518, doi 10.1130/G25462A.1., 2009.

Yeats, R. S.: Active Faults Related to Folding, In Active Tectonics: Impact on Society, The National Academies Press, 280 pp., https://doi.org/10.17226/624, 1986.

Yelding, G., Jackson, J. A., King, G. C. P., Sinvhal H., Vita-Finzi, C., Wood, R. M.: Relations between surface deformation, fault geometry, seismicity, and rupture characteristics during the El Asnam (Algeria) earthquake of the 10 October 1980, Earth Planet. Sci. Lett., 56, 287-304, 1981.

Youngs, Y., W. J. Arabasz, R. R., Anderson, R. E., Ramelli, A. R., Ake, J. P., Slemmons, D. B., McCalpin, J. P., Doser, D. I., Fridrich, C. J., Swan III, F. H., Rogers, A. M., Yount, J. C., Anderson, L. W., Smith, K.

D.,Bruhn, R. L., Knuepfer, L. K., Smith, R. B., dePolo, C. M.,.O'Leary, K.W, Coppersmith, K. J., Pezzopane, S. K., Schwartz, D. P., Whitney, J. W., Olig, S. S., and Toro, G. R.: A methodology for probabilistic fault displacement hazard analysis (PFDHA), Earthq. Spectra 19, 191–219, 2003.

Yu, G. H., Xu, X. W., Chen, G. H., Gou, T. T., Tan, X. B., Yang, H., Gao, X., An, Y. F., and Yuan, R. M.: Relationship between the localization of surface ruptures and building damages associated with the Wenchuan 8.0 earthquake, Chinese J. Geophysics, Vol. 52, No. 6, pp. 1294-1311, 2009.

Yu, G., Xu, X., Klinger, Y., Diao, G., Chen, G., Feng, X., Li, C., Zhu, A., Yuan, R., Guo, T., Sun, X., Tan, X., and An, Y.: Fault-Scarp Features and Cascading-Rupture Model for the Mw 7.9 Wenchuan Earthquake, Eastern Tibetan Plateau, China, Bull. Seismol. Soc. Am., Vol. 100, No. 5B, pp. 2590-2614, 2010.

Zhang, J. Y., Bo, J. S., Xu, G. D., and Huang, J. Y.: Buildings Setbacks Research From Surface-Fault-Rupture Statistical Analysis, Applied Mechanics and Materials, Vols. 204-208, pp. 2410-2418, 2012.

Zhang, Y. S., Shi, J. S., Sun, P., Yang, W., Yao, X., Zhang, C. S., and Xiong T. Y.: Surface ruptures induced by the Wenchuan earthquake: Their influence widths and safety distances for construction sites, Eng. Geol. 166, 245–254, 2013.

Zhang, Y. S., Sun, P., Shi, J. S., Yao, X., and Xiong, T. Y.: Investigation of rupture influenced zones and their corresponding safe distances for reconstruction after 5.12 Wenchuan earthquake, Eng. Geol., 18 (3), 312-319, 2010 (in Chinese with English abstract).

Zhou, Q., Xu, X., Yu, G., Chen, X., He, H., and Yin, G.: Width Distribution of the Surface Ruptures Associated with the Wenchuan Earthquake: Implication for the Setback Zone of the Seismogenic Faults in Post-earthquake Reconstruction, Bull. Seismol. Soc. Am., Vol. 100, No. 5B, pp. 2660-2668, 2010.

Table 1. Earthquakes used for analysing the width of the rupture zone (WRZ).

Earthquake	Date	Magnitude	Kin. #	SRL* (km)	MD* (m)	Depth (km)	References for earthquake parameters (a) and WRZ calculation (b)
1) San Fernando, CA, USA	1971.02.09	M_s 6.5, M_w 6.6	R-LL	16	2.5	8.9 (USGS)	a) 1 b) 2
2) El Asnam, Algeria	1980.10.10	M_s 7.3, M_w7.1	R	31	6.5	10 (USGS)	a) 1 b) 3, 4, 5
3) Coalinga (Nunez), CA, USA	1983.06.11	M_s5.4, M_w 5.4	R	3.3	0.64	2.0 (USGS)	a) 1 b) 6
4) Marryat Creek, Australia	1986.03.30	M_s 5.8, M_w 5.8	R-LL	13	1.3	3.0	a) 1, 7 b) 8, 9
5) Tennant Creek, Australia	1988.01.22 (3 events)	M_s 6.3, M_w 6.3 M_s 6.4, M_w 6.4 M_s 6.7, M_w 6.6	R R-LL R	10.2 6.7 16	1.3 1.17 1.9	2.7 3.0 4.2	a) 1, 10 b) 11
6) Spitak, Armenia	1988.12.07	M_s 6.8, M_w 6.8	R-RL	25	2.0	5.0-7.0	a) 1, 12 b) 13
7) Killari, India	1993.09.29	M_s 6.4, M_w 6.2	R	5.5	0.5	2.6	a) 14, 15 b) 15, 16
8) Chi Chi, Taiwan	1999.09.20	M_w 7.6	R-LL	72	12.7	8.0	a) 17, 18 b) 19, 20, 21, 22, 23, 24, 25, 26, 27, 28, 29, 30, 31, 32, 33, 34, 35, 36, 37, 38, 39, 40, 41
9) Kashmir, Pakistan	2005.10.08	M_w 7.6	R	70	7.05 (v)	<15.0	a) 42, 43 b) 43, 44
10) Wenchuan, China	2008.05.12	M_w 7.9	R-RL	240	6.5 (v) 4.9 (h)	19.0 (USGS)	a) 45 b) 46, 47, 48, 49, 50, 51, 52, 53, 54, 55, 56, 57, 58, 59
11) Nagano, Japan	2014.11.22	M_w 6.2	R	9.3	1.5 (v)	4.5	a) 60, 62 b) 60, 61, 62

Commento [UW10]: New data (see comments from Rev. 2)

Kin. (kinematics): R = reverse, LL = left lateral, RL = right lateral.
* SRL = surface rupture length; MD = maximum displacement (vector sum, unless otherwise specified; v = vertical; h = horizontal).
References: 1 = Wells and Coppersmith, 1994; 2 =U.S. Geological Survey Staff, 1971; 3 =Yelding et al., 1981; 4 =Philip and Meghraoui, 1983; 5 =Meghraoui et al 1988; 6 = Rymer et al. 1990; 7 = Fredrich et al., 1988; 8 = Bowman and Barlow, 1991; 9 = Machette et al., 1993; 10 = McCaffrey, 1989; 11 = Crone et al., 1992; 12 = Haessler et al. 1992; 13 = Philip et al. 1992; 14 = Lettis et al., 1997; 15 = Seeber et al. 1996; 16 = Rajendran et al., 1996; 17 = Wesnousky, 2008; 18 = Shin and Teng, 2001; 19 = Kelson et al., 2001; 20 = Kelson et al., 2003; 21 = Angelier et al., 2003; 22 = Bilham and Yu, 2000; 23 = Chang and Yang, 2004; 24 = Chen et al., 2000; 25 = Chen et al., 2003; 26 = Faccioli et al., 2008; 27 = Huang et al., 2008; 28 = Huang et al., 2000; 29 = Huang, 2006; 30 = Kawashima, 2002; 31 = Konagai et al., 2006; 32 = Lee and Loh, 2000; 33 = Lee et al., 2001; 34 = Lee and Chan, 2007; 35 = Lee et al., 2003; 36 = Lee et al., 2010; 37 = Lin, 2000; 38 = Ota et al., 2001; 39 = Ota et al., 2007a; 40 = Ota et al., 2007b; 41 = Central Geological Survey, MOEA at http://gis.moeacgs.gov.tw/gwh/gsb97-1/sys8/index.cfm; 42 = Avouac et al., 2006; 43 = Kaneda et al., 2008; 44 = Kumahara and Nakata, 2007; 45 = Xu et al., 2009; 46 = Liu-Zeng et al., 2009; 47 = Liu-Zeng et al., 2012; 48 = Yu et al., 2009; 49 = Yu et al., 2010; 50 = Zhou et al., 2010; 51 = Zhang et al., 2013; 52 = Chen et al., 2008; 53 = Dong et al., 2008a; 54 = Dong et al., 2008b; 55 = Liu-Zeng et al., 2010; 56 = Wang et al., 2010; 57 = Xu et al., 2008; 58 = Zhang et al., 2012; 59 = Zhang et al., 2010; 60 = Okada et al., 2015; 61 = Ishimura et al., 2015; 62 = Lin et al., 2015.

Table 2 - Width of the rupture zone (WRZ) on the hanging wall (HW) and on the footwall (FW) and FW to HW ratio for (a) "simple thrust" distributed ruptures (B-M, F-S and Sy excluded) and (b) all distributed ruptures.

(a)

Probability[1]	WRZ **HW**	WRZ **FW**	**Total** WRZ	**FW:HW**
90%	575 m	265 m	840 m	1:2.2
75%	260 m	120 m	380 m	1:2.2
50%	80 m	45 m	125 m	1:1.8
35%[2]	40 m	20 m	60 m	1:2

(b)

Probability[1]	WRZ **HW**	WRZ **FW**	**Total** WRZ	**FW:HW**
90%	1100 m	720 m	1820 m	1:1.5
75%	640 m	330 m	970 m	1:1.9
50%	260 m	125 m	385 m	1:2.1
35%[3]	130 m	65 m	195 m	1:2

Commento [UW11]: New table (see comments from Rev.s 1 and 2)

[1] Probabilities refer to the cumulative distribution functions of Fig.s 4 and 5.
[2] Corresponding to a sharp drop of data in the histograms of Fig. 4, close to the principal fault.
[3] Calculated for comparison with "simple thrust" database, but not corresponding to particular drops of data in the histograms of Fig. 5.

Table 3 Comparison between fault zone size from Italian guidelines and the Width of the Rupture Zone (WRZ) from the present study (proposal for integrating fault zoning for thrust faults). PF = principal fault rupture; DR = distributed ruptures; SFRH = surface fault rupture hazard.

ZONE[1]	**Seismic Microzonation**[2]	**Italian guidelines**	**Proposed widths of zones from total WRZ (from "simple thrust" DR**[3]**)**	**Total WRZ from all DR (including B-M, F-S and Sy)**	**FW:HW**[5]
Warning Zone (*Zona di attenzione, ZA*)	Basic (Level 1)	400 m (FW:HW = 1:2)	**> 380 m** (minimum; 75% prob.) to **840 m** (recommended; 90% prob., all the reasonably inferred hazard from PF and DR)	**1800 m** (90% prob., applicable in poorly-known areas for assessing the extent of potential SFRH)	1:2
Avoidance Zone (*Zona di rispetto*, ZR)	High-level (Level 3)	30 m (FW:HW = 1:2)	**60 m** (35% prob.[4], very high hazard)		1:2
Susceptible Zone (*Zona di suscettibilità*, ZS)	High-level (Level 3)	160 m (FW:HW = 1:2)	**Variable** (depending on the detail of Level 3 MS and structural complexity) **380 m** (in the absence of particular constraints; 75% prob., precautionary)		1:2

[1] The original names of zones in the Italian guidelines (in Italian) are in italics.
[2] Different levels of Seismic Microzonation refer to SM Working Group (2015).
[3] B-M, F-S and Sy fault ruptures are not included.
[4] Corresponding to a sharp drop of data in the histograms of Fig. 4.
[5] The computed values (Table 2) have been simplified to 1:2.

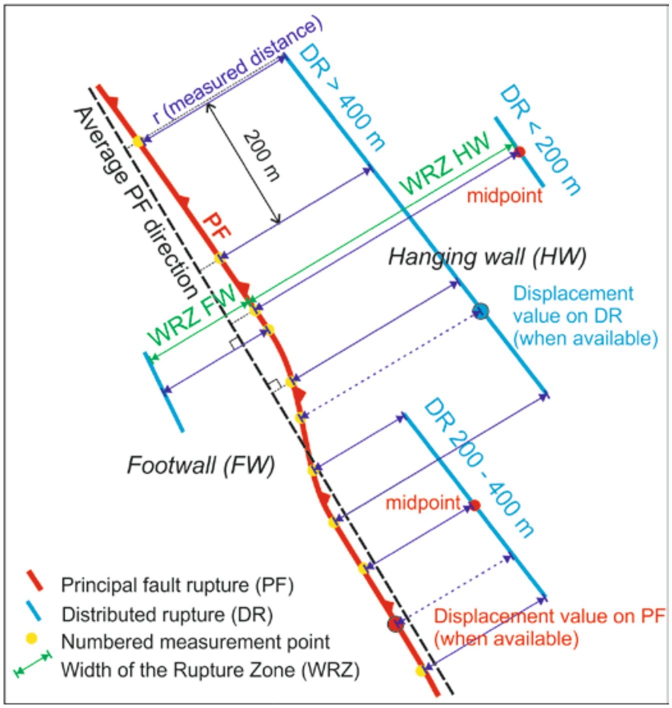

Figure 1 Sketch synthesizing the methodology used for measuring the "r" and WRZ data. Distance between the principal fault rupture and distributed rupture is measured along the line perpendicular to the auxiliary line indicating the average direction of the principal fault, always between the faults. Points with displacement values are prioritised at the expense of the 200 m metrics (the closest measurement point) when reasonable, in order to avoid over measuring.

Commento [UW12]: Update figure.
Comment 2 of Rev. 1
Comment 2 of Rev. 2

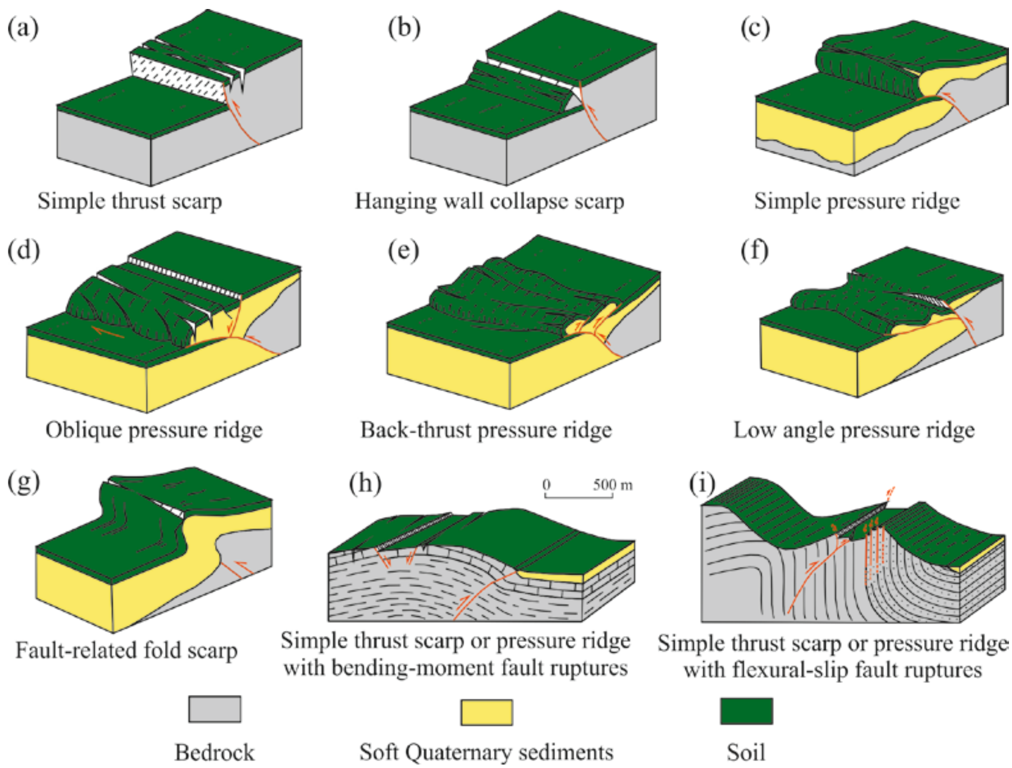

Figure 2 Scarp type classification (modified after Philip et al., 1992 and Yu et al., 2010). The scarp types h) and i) are associated with large-scale folds (hundreds of meters to kilometres in wavelength) and are from Philip and Meghraoui (1983).

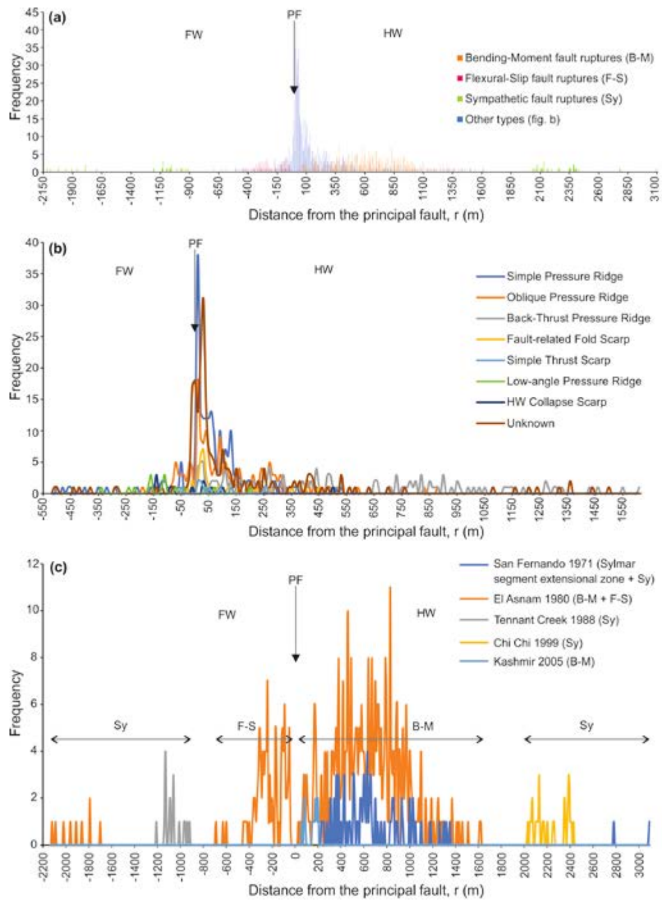

Figure 3 a) Frequency distribution histogram of the distributed ruptures distance (r) from the principal fault rupture (PF) for the earthquakes reported in Table 1. The positive and negative values refer to the data on the hanging wall and the footwall, respectively; b) Frequency distribution curves of each scarp type excluding those associated with B-M, F-S and Sy fault ruptures (types h and i of Fig. 2 and sympathetic slip triggered on distant faults); c) Frequency distribution curves of the B-M, F-S and Sy fault ruptures distinguished by earthquakes (the Sylmar segment extensional zone of the San Fernando 1971 earthquake rupture is included into the B-M fault ruptures).

Commento [UW13]: Updated figure

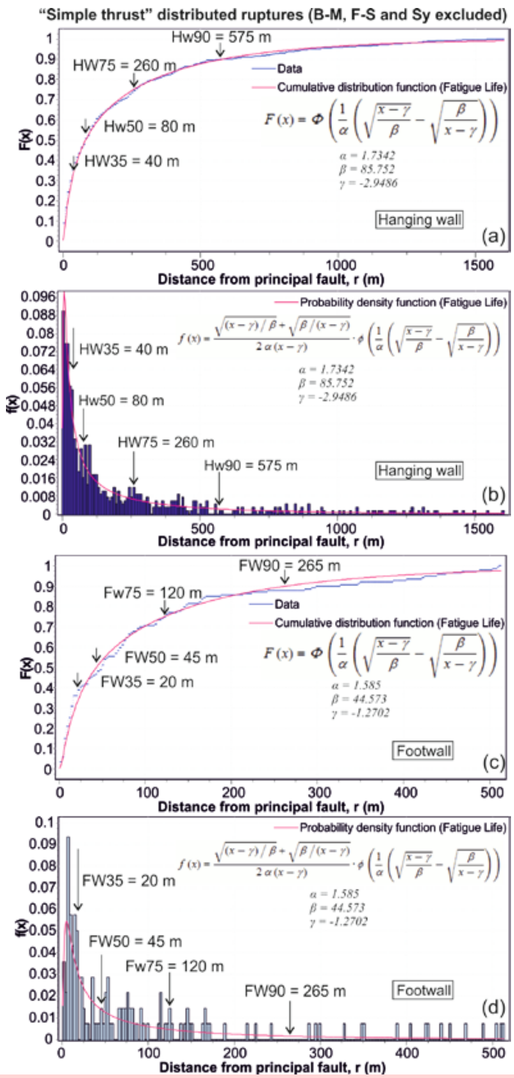

Figure 4 Cumulative distribution function and probability density function of the rupture distance (r) from the PF for the hanging wall (a and b, respectively) and the footwall (b and c, respectively) of the PF. Only the scarp types without associated B-M, F-S or sympathetic fault ruptures ("simple thrust" distributed ruptures) were analysed. The 35% probability (HW35) is indicated because it corresponds to sharp drop of the data in the histograms.

Commento [UW14]: Updated figure

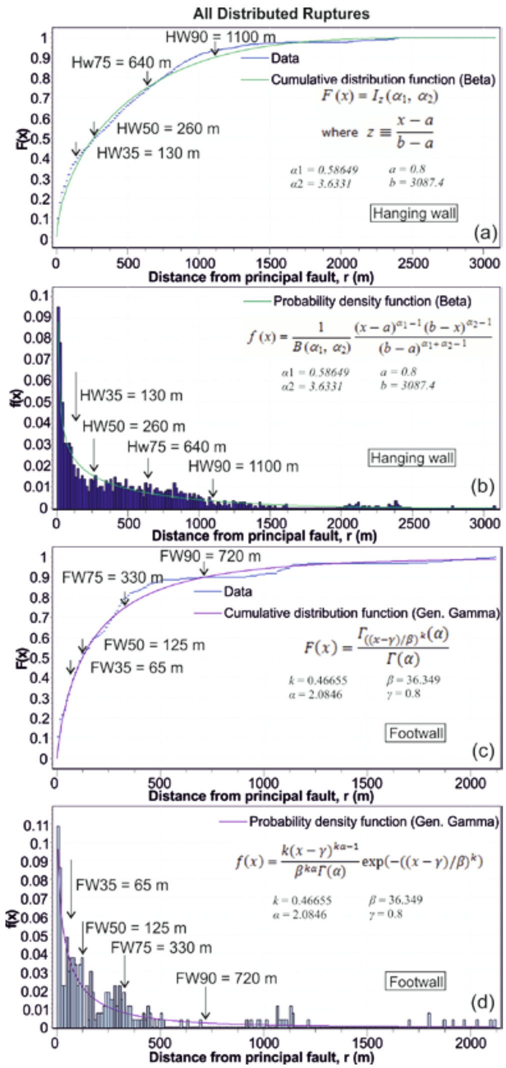

Figure 5 Cumulative distribution function and probability density function of the rupture distance (r) from the PF for the hanging wall (a and b, respectively) and the footwall (c and d, respectively) of the PF. All types of distributed ruptures were considered. The 35% probability (HW35) is indicated for comparison with "simple thrust" database (Fig. 4), but it does not correspond to particular drops of the data in the histograms.

Commento [UW15]: New figure. Comment 3 of Rev. 1 Comment 1 of Rev. 2

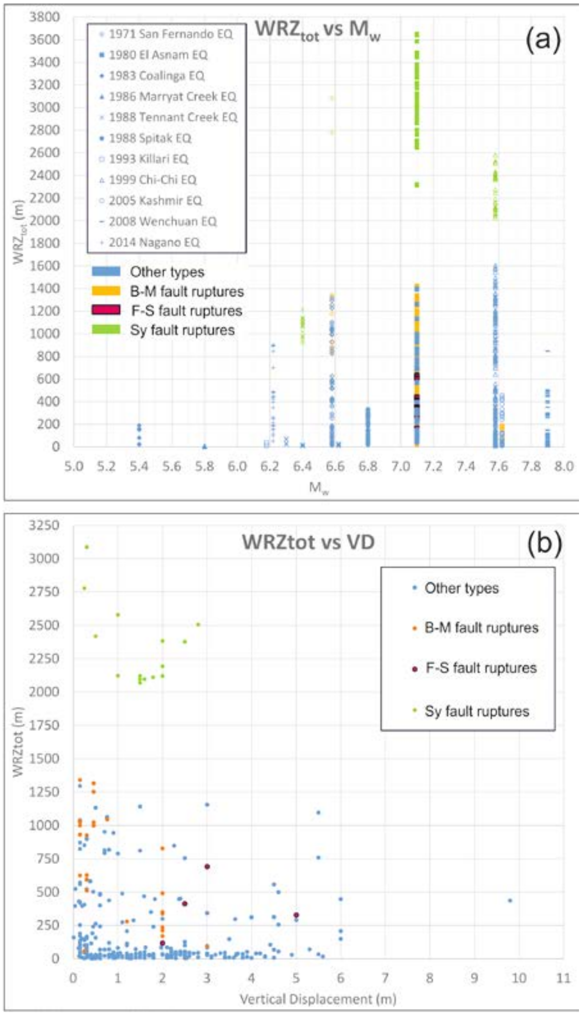

Figure 6 a) Diagram plotting the total WRZ (WRZtot = WRZ hanging wall + WRZ footwall) against (a) the earthquake magnitude (Mw) and (b) the vertical displacement (VD) on the principal fault.

Commento [UW16]: Modified figure. Comments from Rev.s 1 and 2

Width of surface rupture zone for thrust earthquakes. Implications for earthquake fault zoning.

Paolo Boncio[1], Francesca Liberi[1], Martina Caldarella[1], Fiia C.Nurminen[2]

[1]CRUST-DiSPUTer,“G. D’Annunzio” University of Chieti-Pescara, Chieti, I-66100, Italy

[2]Oulu Mining School, University of Oulu, Oulu, FI-90014, Finland

Correspondence to: Paolo Boncio (paolo.boncio@unich.it)

Abstract. The characteristics of the zones of coseismic surface faulting along thrust faults are analysed in order to define the criteria for zoning the Surface Fault Rupture Hazard (SFRH) along thrust faults. Normal and strike-slip faults have been deeply studied by other authors~~in the past~~ concerning the SFRH, while thrust faults have not been studied with comparable attention.

Surface faulting data were collected from ~~10~~ 11 well-studied historic thrust earthquakes occurred globally (5.4 ≤ M ≤ 7.9). Several different types of coseismic fault scarps characterise the analysed earthquakes, depending on the topography, fault geometry and near-surface materials (simple and hanging wall collapse scarps; pressure ridges; fold scarps and thrust or pressure ridges with bending-moment or flexural-slip secondary faults due to large-scale folding). For all the earthquakes, the distance of ~~secondary~~ distributed ruptures from the ~~main~~ principal fault rupture (r) and the width of the rupture zone (WRZ) were compiled directly from the literature or measured systematically in GIS-georeferenced published maps.

Overall, surface ruptures can occur up to large distances from the main fault (~~~750~~ 2,150 m on the footwall and ~~~1,6~~3,100 m on the hanging wall). Most of them occur on the hanging wall, preferentially in the vicinity of the ~~main~~ principal fault trace (> 50% at distances <~ ~~50~~ 250 m). The widest WRZ are recorded where sympathetic slip (Sy) on distant faults occurs, and/or where bending-moment (B-M) or flexural-slip (F-S) ~~secondary~~ fault ruptures, associated ~~to~~ with large-scale folds (hundreds of meters to kilometres in wavelength), are present.

A positive relation between the earthquake magnitude and the total WRZ is evident, while a clear correlation between the vertical displacement on the principal fault and the total WRZ is not found.

The distribution of surface ruptures is fitted with probability density functions, in order to define a criterion to remove outliers (e.g. 90% probability of the cumulative distribution function) and define the zone where the likelihood of having surface ruptures is the highest. This might help in sizing the zones of SFRH during seismic microzonation (SM) mapping.

In order to shape zones of SFRH, a very detailed earthquake geologic study of the fault is necessary (the highest level of SM, i.e., Level 3 SM according to Italian guidelines). In the absence of such a very detailed study (basic SM, i.e., Level 1 SM of Italian guidelines) a width of ~~~465~~ 840 m (90% probability from “simple thrust” database of distributed ruptures, excluding B-M, F-S and Sy ruptures) ~~seems~~ is suggested to be ~~adequate~~sufficiently precautionary. For more detailed ~~level~~ SM, where the fault is carefully mapped, one must consider that the highest SFRH is concentrated in a narrow zone, ~60 m~~only 50-70~~ in width , that should be considered as a fault avoidance zone (~~40-50%~~more than one third of the ~~total~~ distributed ruptures are expected to occur within this zone).

~~A broad positive relation between the displacement on the main fault and the total width of the rupture zone is found only close to the main fault (total WRZ ≤ 60 m). The total WRZ appears to increase with displacement, from a minimum of nearly 20-30 m for decimetric vertical displacement up to 50-60 m for vertical displacement close to 2 m.~~

The fault rupture hazard zones should be asymmetric compared to the trace of the ~~main~~ principal fault. The average footwall to hanging wall ratio (FW: HW) is close to 1:2.

These criteria are applicable to “simple thrust ~~faults~~” faults, without considering possible B-M or F-S ~~secondary~~ fault ruptures ~~on~~ due to large-scale ~~folds~~folding, and without considering sympathetic slip on distant faults. ~~Zones~~ Areas potentially susceptible to B-M or F-S ~~secondary~~ fault ruptures should have their own zones of fault rupture hazard that can be ~~inferred~~ defined by detailed knowledge of the structural setting of the area (shape, wavelength, tightness~~geometry, wavelength~~ and lithology of the thrust-related large-scale folds) and by geomorphic evidence of past secondary faulting. Distant active faults, potentially susceptible to sympathetic triggering, should be zoned as separate principal faults.

The entire database of distributed ruptures (including B-M, F-S and Sy fault ruptures) can be useful in poorly-known areas, in order to assess the extent of the area within which potential sources of fault displacement hazard can be present.

The results from this study and the database made available as supplementary material can be used for improving the attenuation relationships for distributed faulting, with possible applications in probabilistic studies of fault displacement hazard.

Key words

Fault rupture hazard, thrust earthquakes, earthquake fault zoning.

1 Introduction

Coseismic surface ruptures during large earthquakes might produce damage to buildings and facilities located on or close to the trace of the active seismogenic fault. This is known as Surface Fault Rupture Hazard (SFRH), a localized hazard that could be avoided if a detailed knowledge of the fault characteristics is achieved. The mitigation of SFRH can be faced by strategies of fault zoning and avoidance or, alternatively, by (or together with) probabilistic estimates of fault displacement hazard (e.g. Youngs et al., 2003; Petersen et al., 2011). Both strategies need to employ, as accurately as possible, the location of the active fault trace, the expected displacement on the ~~main~~ principal fault (i.e. *principal faulting* in Youngs et al., 2003; see below for the definition), the deformation close to the ~~main~~ principal fault, and the distribution of ~~secondary~~ other faulting and fracturing away from it (i.e. *distributed faulting* in Youngs et al., 2003; see below for the definition). While the general ~~fault~~ geometry and the expected displacement of the principal fault can be obtained through a detailed geological study and the application of empirical relationships (e.g. Wells and Coppersmith, 1994), the occurrence of ~~secondary~~ distributed faulting close to and away from the ~~main~~ principal fault rupture is particularly difficult to predict, and only direct observations from well-documented case studies may provide insights on how ~~secondary~~ distributed faulting is expected to occur (e.g. shape and size of rupture zones, attenuation relationships for ~~secondary~~ distributed faulting).

A reference example of fault zoning strategy for mitigating SFRH is the Alquist-Priolo Earthquake Fault Zoning Act (A-P Act), adopted by the state of California (USA) in 1972 (e.g. Bryant and Hart, 2007). The A-P Act defines regulatory zones around active faults (Earthquake Fault Zones, EFZ), within which detailed geologic investigations are required prior to build structures for human occupancy. The boundaries of the EFZ are placed 150-200 m away from the trace of major active faults, or 60 to 90 m away from well-defined minor faults, with exceptions where faults are complex or not vertical. Moreover, the A-P Act defines a minimum distance of 50 feet (15 m) from the well-defined fault trace within which ~~critical facilities and~~ structures designed for human occupancy cannot be built (fault setback), unless proven otherwise. Similarly ~~to the setback of the A-P Act~~, the New Zealand guidelines for development of land on or close to active faults (Kerr et al., 2003) define a fault avoidance zone to ensure life safety. Fault avoidance zones on district planning maps will allow a council to restrict development within the fault avoidance zone and take a risk-based approach to development in built-up areas. The risk-based approach combines the key elements of fault recurrence interval, fault complexity and building importance category. The guidelines recommend a minimum buffer of 20 m either sides of the known fault trace (or the likely rupture zone), unless detailed fault studies prove that the deformed zone is less than that.

Recently, in Italy the Department for Civil Protection published guidelines for land management in areas affected by active and capable faults. For the purpose of the guidelines, an active and capable fault is defined as a fault with demonstrated evidence of surface faulting during the last 40,000 years (Technical Commission for Seismic Microzonation, 2015; SM Working Group, 2015). The guidelines are a tool for zoning active and capable faults during seismic microzonation (SM). They also contain a number of recommendations to assist land managers and planners. The fault zones vary at different Levels of SM. In the basic SM (Level 1 SM according to SM Working Group, 2015), the active fault is zoned with a wide Warning Zone that is conceptually equivalent to the EFZ of the A-P Act. The zone should include all the reasonable inferred fault-rupture hazard of both the ~~main~~ principal fault and other secondary faults, and should account for uncertainties in mapping the fault trace. The guidelines recommend a width of the Warning Zone to be 400 m. Within the Warning Zone, the most detailed level of SM (Level 3 SM) is recommended; this should be mandatory before new development~~construction~~. Level 3 SM implies a ~~very~~ detailed earthquake geology study of the fault. After completing that study, a new, more accurate fault zoning is achieved. This includes a 30 m-wide Fault Avoidance Zone around the accurately-defined fault trace. If some uncertainties persist after Level 3 studies, such as uncertainties about fault trace location or about the possibility of secondary faulting away from the ~~main~~ principal fault, the guidelines suggest the use of a wider zone called Susceptible Zone, within which development is restricted. Uncertainties within the Susceptible Zone can be reduced by additional site-specific investigations. The guidelines recommend a width of the Susceptible Zone to be 160 m, but the final shape and size of the zone depend on the local geology and the level of accuracy reached during Level 3 SM studies. Both Fault Avoidance and Susceptible Zones can be asymmetric compared with the main fault trace, with recommended footwall to hanging wall ratios of 1:4, 1:2 and 1:1 for normal, thrust and strike-slip faults, respectively.

Shape and width of the zones in the Italian guidelines are based mostly on data from normal faulting earthquakes (e.g. Boncio et al., 2012). In general, ~~worldwide the width of the rupture zone (WRZ) for~~ the fault displacement hazard ~~normal~~of normal and strike-slip ~~earthquakes~~ faults (e.g. Youngs et al., 2003; Petersen et al., 2011) ~~is~~ has been much more studied than that of ~~for~~ thrust faults~~earthquakes~~. Zhou et al. (2010) analysed the width of the surface rupture zones of the 2008 Wenchuan earthquake focusing on the rupture zone close to the ~~main~~ principal fault, with implications on the setback distance. However, to our knowledge, a global data ~~collection~~ compilation from well-documented surface thrust faulting earthquakes aimed at analysing the characteristics of the WRZ is lacking in the scientific literature.

The objectives of this work are: 1) to ~~collect the~~compile data from well-studied surface faulting thrust earthquakes globally (we analysed ~~10~~ 11 earthquakes with magnitudes ranging from 5.4 to 7.9); 2) to analyse statistically the distribution of surface ruptures compared to the ~~main~~ principal fault and the associated WRZ; and 3) to compare the results with the ~~contemporary~~ Italian guidelines and discuss the implications for earthquake fault zoning.

2 Methodology

This work analyses the data from ~~10~~ 11 well-studied historic surface faulting thrust earthquakes occurred worldwide during the last few decades (Table 1). These historic earthquakes range in magnitude (Mw) from 5.4 to 7.9 and belong to different tectonic settings, such as continental collision (Spitak, 1988; Kashmir, 2005; Wenchuan, 2008), fold-and-thrust belt (El Asnam, 1980), oceanic-continental or continental-continental collision in large-scale subduction systems (Chi-Chi, 1999; Nagano, 2014), transform plate boundary (San Fernando, 1971; Coalinga-Nunez, 1983) and intraplate regions (Marryat Creek, 1986; Tennant Creek, 1988; Killari, 1993).

We compiled from the literature data on both principal and distributed faulting, as defined by Youngs et al. (2003). Principal faulting is displacement along the main fault responsible for the release of seismic energy during the earthquake. At the surface, the displacement may occur along a single narrow trace of the principal fault or within a meters-scale wide fault zone. Distributed faulting is displacement on other faults in the vicinity of the principal fault rupture. Distributed ruptures are often discontinuous and may occur tens of meters to kilometers away from the principal fault rupture. Displacement may occur on secondary faults connected with the principal fault, such as splay faults, or on pre-existing faults structurally unconnected with the main fault (called here sympathetic fault ruptures). In particular, f~~F~~or the purpose of this work, the following parameters were ~~collected~~ extracted from the literature listed in Table 1: i) displacement (vertical, horizontal and net slip, if available) on the ~~main~~ principal fault rupture and coordinates of the referred measurement points for strands of the principal fault having associated distributed ruptures; ii) distance from the ~~main~~ principal fault to the ~~secondary~~ distributed ruptures (r in Fig. 1), distinguishing between the ones on hanging wall and on footwall; iii) displacement on distributed ruptures ~~secondary faults~~ (if available); iv) width of the rupture zone (WRZ), distinguishing between the ones on hanging wall and on footwall; and v) scarp type (Fig. 2).

When available, the surface rupture data was ~~collected~~ compiled directly from ~~the literature~~published tables (e.g., Chi-Chi, 1999; Wenchuan, 2008), but in most of the other cases the rupture data was measured from the ~~published~~ maps published by the previous authors that were GIS-georeferenced for the purpose of this work. Figure 1 displays the technique used for measuring the distance between the ~~main~~ principal fault rupture (PF) and the ~~secondary~~ distributed ruptures (DR), which allowed us to sample the rupture zone systematically and in reasonable detail. The measurements carried out on the published maps are illustrated in Fig.s S1 to S11 of the online supplementary material, and the entire compiled database is made available in Table S1. The accuracy of the measurements depends on the scale of the original maps and on the level of detail reported in the maps (the original scale of the published maps is reported in the figures of the supplementary material). In this work only detailed maps were considered, and uncertain or inferred ruptures were not taken into account. It is important to specify that the database made available in Table S1 of the supplementary material can be used only for analysing distributed faulting. Data on the principal fault rupture are not complete, because the strands of the principal fault without distributed ruptures were not considered.

In order to distinguish the principal fault rupture from distributed ruptures, all of the following were considered: 1) larger displacement compared to distributed faulting; 2) longer continuity; 3) coincidence or nearly coincidence with major tectonic/geomorphologic features, such as the trace of the main fault mapped before the earthquake on geologic maps.

The distance was measured perpendicularly to the average direction of the principal fault, which was defined by visual inspection of the published maps, averaging the direction of first-order sections of the principal fault rupture (few to several km-long). Particular attention was paid close to variations of the average strike, in order to avoid duplicate measurements. In some places, the principal fault rupture is discontinuous. In few of those cases, and only for the purpose of measuring the distance of distributed ruptures from the main fault trace, we drew the trace of the main geologic fault between nearby discontinuous ruptures by using major tectonic/geomorphologic features from available maps (inferred trace of the principal geologic fault in Fig.s S1, S2, S8, S9, S10 and S11).

Distributed ruptures were measured every 200 m along-strike the principal fault. In order to prevent that short ruptures would be missed or under-sampled during measurement, ruptures shorter than 200 m were measured at the midpoint, and ruptures between 200 and 400 m-long were measured at the midpoint and endpoints (Fig. 1). Moreover, all the points having displacement information on distributed ruptures were measured. All the points with displacement values on the principal fault rupture were also measured if distributed ruptures were associated with that strand of the principal fault. A particular metrics was used for the Sylmar segment of the San Fernando 1971 rupture zone (Fig. S1) where most of the distributed faulting was mapped along roads, resulting in a very discontinuous pattern of surface ruptures. In order to have a database of measurements statistically equivalent respect to the other studied earthquakes, variable measurement logics were used in order to sample ruptures at distances that equal more or less 200 m (see Fig. S1 for details).

All the distributed ruptures reported in the published maps as of primary (i.e., tectonic) origin were measured. Only the “Beni Rached” rupture zone of the 1981 El Asnam earthquake (Fig. S2) was not measured. It consists of normal fault ruptures interpreted to be related to either or both (Yelding et al., 1981; Philip and Meghraoui, 1983): 1) very large gravitational sliding; and 2) surface response of an unconstrained deep tectonic fault also responsible for the 1954 M 6.7 earthquake. Therefore, we avoided measuring the rupture due to the large uncertainties concerning its primary origin.

Some distributed ruptures reasonably unconnected with the main seismogenic fault were classified as sympathetic fault ruptures (Sy; Figs. S1, S2 and S5). We included in this category a rupture on a pre-existing thrust fault located more than 2 km in the hanging wall of the Chi-Chi 1999 principal fault rupture, due to its large distance from the main fault trace compared to all the other distributed ruptures (Tsauton East fault, Fig. S8), but a deep connection with the main seismogenic fault is possible (Ota et al., 2007a). ~~The accuracy of the measurements depends on the scale of the original maps and on the level of detail reported in the maps. In this work only the detailed maps were considered, uncertain or inferred ruptures were not taken into account.~~

The measured ruptures have been classified according to the scarp types illustrated in Fig. 2, alternatively the scarp type was classified as “Unknown”. Scarp types from “a” to “g” (Fig. 2) follow the scheme proposed by Philip et al. (1992), integrated with the classification of Yu et al. (2010). ~~Concerning the scarp type, thrust earthquakes are characterized by a high variability of coseismic scarps due to the complex interaction between faulting and folding, geometry of the faults, and topography and rheology of the surface materials. The coseismic scarps can be classified according to the scheme first proposed by Philip et al. (1992) after the 1988 Spitak (Armenia) earthquake, integrated with the classification of Yu et al. (2010), which includes seven main types of thrust-related fault scarps and related secondary structures (Fig. 2).~~ In case of steeply dipping faults, a simple thrust scarp in bedrock (type a) or a hanging wall collapse scarp in bedrock or in brittle unconsolidated material (type b) are produced. In case of low-angle faults and presence of soft-sediment covers, ~~a number of~~various types of pressure ridges (types c to f) can be observed, depending on the displacement, sense of slip and behaviour of near-surface materials. In presence of shallow blind faults, a fault-related fold scarp may be formed (type g). Moreover, in this study ~~also~~ two additional ~~types of thrust scarps~~structural contexts were distinguished, which are characterized by the occurrence of bending-moment and flexural-slip ~~secondary~~ fault ruptures (Yeats, 1986), associated with large-scale folds (hundreds of meters to kilometres in wavelength). Both of ~~them~~ these occurred widely during the 1980 El Asnam earthquake (Philip and Meghraoui 1983). Bending-moment faults (type h in Fig. 2) are normal faults that are formed close to the hinge zone of large-scale anticlines (extensional faults at the fold extrados in Philip and Meghraoui 1983), while flexural-slip faults (type i) are faults that are formed due to differential slip along bedding planes on the limbs of a bedrock fold (Yeats, 1986). Similar secondary Bending-moment distributed ruptures associated to with small-scale folds (meters to dozens of meters in wavelength), which form at the leading edge of the thrust, are not included in these two particular typesbelong to scarp types “c” to “g”. The measured rupture data has been classified according to the scarp types illustrated in Fig. 2 whenever possible; alternatively, the scarp type was classified as “Unknown”.

3 Width of the Rupture Zone (WRZ): statistical analysis

The most impressive and recurrent measured features are ruptures occurring along pre-existing fault traces and on the hanging wall, as the result of the reactivation of the main thrust at depth. Secondary structuresDistributed ruptures are mainly represented by synthetic and antithetic faults, which are parallel to or branching from the main fault. Fault segmentation and en échelon geometries are common in transfer zones or in oblique-slip earthquakes.

The collected data was analysed in order to evaluate the width of the rupture zone (WRZ), intended as the total width, measured perpendicularly to the main faultprincipal fault rupture, within which all the secondary distributed ruptures occur. Figure 3 shows frequency distribution histograms of the distance of distributed rupturessecondary ruptures from the main principal fault (r) for all the analysed earthquakes. Negative values refer to the footwall, while positive values refer to the hanging wall. In particular, in Fig. 3a we distinguished the scarps with bending-moment (B-M), or flexural-slip (F-S) or sympathetic (Sy) secondary fault ruptures from the other types; in Fig. 3b the scarps without B-M, or F-S or Sy secondary fault ruptures are distinguished by scarp types, and in Fig. 3c the scarps with B-M, or F-S or Sy secondary fault ruptures are distinguished by earthquake. In general, although the values span over a large interval (-750 2,150 m to in the footwall; 1,6103,100 m in the hanging wall), most of them occur in the proximity of the main principal fault and display an asymmetric distribution between hanging wall and footwall.

In Fig. 3b all the data (excluding scarps with B-M, and F-S and Sy faults) are distinguished by scarp type. Simple Pressure Ridges with narrow WRZ (in green) prevail. Larger WRZ characterizes back-thrust, low-angle and oblique pressure ridges, and the relative data, together with those associated to the other pressure ridges (oblique, back-thrust and low-angle), span over an interval that is larger than for simple thrust scarps (in blue). This im-

~~plies~~ implying that the main thrust geometry, the local kinematics and the near-surface rheology have a significant control in strain partitioning with consequences on the WRZ, as expected.

The occurrence of B-M or F-S ~~secondary~~ fault ruptures is strictly related to the structural setting of the earthquake area. In particular, B-M faults, which are related to the presence of large-scale hanging wall anticlines, were clearly observed in the El Asnam 1980 (Philip and Meghraoui, 1983) and Kashmir 2005 (southern part of central segment; Kaneda et al., 2008; Sayab and Khan, 2010) earthquakes. A wide extensional zone (1.8 km-long in the E-W direction; 1.3 km-wide) formed on the eastern hanging wall side of the Sylmar segment of the San Fernando 1971 surface rupture. The interpretation of such an extensional zone is not straightforward. Nevertheless, the presence of a macro-anticline in the hanging wall of the Sylmar fault is indicated by subsurface data (Mission Hill anticline; Tsutsumi and Yeats, 1999). Though it is not possible to clearly classify these structures as B-M faults in strict sense, it seems reasonable to interpret them as generic fold-related secondary extensional faults. Therefore, they were plotted in Fig.s 3a and 3c together with B-M ~~and F-S~~ faults. F-S faults were observed on the upright limb of a footwall syncline in the El Asnam 1980 earthquake. ~~As shown in Fig. 3a, the B-M and F-S datasets contribute significantly in widening the WRZ and are distributed only on the hanging wall or on the footwall of the main fault, respectively. Notably, the distribution of the B-M faults for the El Asnam earthquake is very similar to the distribution of extensional ruptures for the San Fernando earthquake (Fig. 3c).~~ Ruptures close to the main fault (r < ~~200~~ 150 m) are due to processes operating in all the ~~other types of~~ scarp types (Fig. 3b), but for larger distances ~~(r > ~300 m) they~~ the distributed faulting can be affected by other processes such as ~~related to~~ large-scale folding ~~of a large-scale anticline~~or sympathetic reactivation of pre-existing faults (Fig.s 3a and 3c), contributing significantly in widening the WRZ. ~~with a larger frequency between 300 and 1,000 m from the main fault. The B-M ruptures for the Kashmir 2005 earthquake are localized in a narrower zone (≤ 200 m) closer to the main fault, due to the shorter wavelength of the hosting anticline.~~

~~In order to analyse~~For the analysis of the statistical distribution of “r”, the collected data was fitted with a number of probability density functions by using the commercial software EasyFitProfessional©V.5.6 (http://www.mathwave.com), which finds the probability distribution that best fits the data and automatically tests the goodness of the fitting. We decided to analyse both the database without B-M, F-S and Sy ruptures (called here “simple thrust” distributed ruptures; Fig. 4) and the entire database of distributed ruptures without filtering (Fig. 5). The aim is to analyse separately: 1) distributed ruptures that can be reasonably related only to (or preferentially to) the coseismic propagation to the ground surface of the main fault rupture; they are expected to occur in a rather systematic way compared to the main fault trace; and 2) distributed ruptures that are affected also by other, non-systematic structural features, mostly related to large-scale coseismic folding. ~~Considering that~~

~~the width of the rupture zone for the scarps with B-M and F-S is strictly related to the structural setting of the area (presence and wavelength of the fold)~~, ~~in this study only the scarp types without B-M and F-S (called here “simple thrust ruptures”) were analysed. The aim is to find a criterion for removing the outliers and sizing the zones within which surface fault ruptures are expected to occur.~~ The hanging wall and footwall data ~~was~~ were fitted separately and the results are synthesized in Fig.s 4 and 5, where the best fitting distribution curves and the cumulative curves~~, selected by the software according to the Kolmogorov-Smirnov test,~~ are shown. ~~The same continuous function was found for both the hanging wall and footwall, which is the Birnbaum-Saunders (Fatigue Life) distribution.~~

For “simple thrust” distributed ruptures, ~~The~~ the hanging wall data (Figs. 4a and 4b) has a modal value of ~~5.5~~7.1 m. The 90% probability (0.9 of the cumulative distribution function, HW90) seems to be a reasonable value to cut off the outliers (flat part of the curves). It corresponds to a distance of ~~~320~~ 575 m from the ~~main~~ principal fault. From a visual inspection of the ~~The~~ histogram (Fig. 4b), there is an evident sharp drop of the data approximately at the 35% probability (HW35), corresponding to a distance of ~40 m from the principal fault. ~~shows a zone close to the main fault, bounded by the 40% probability, where most of the ruptures occur (HW40, corresponding to ~30 m from the main fault)~~. ~~A~~ The second sharp drop of the data in the histogram occurs ~~at~~ close to the 50% probability (HW50, corresponding to ~~~45~~ 80 m from the ~~main~~ principal fault). Also the 3rd quartile is shown (HW75), corresponding to a distance of ~~~140~~ 260 m from the main fault. The widths of the zones for the different probabilities (90%, 75%, 50% and ~~40~~35%) are listed in Table 2a.

The footwall data (Figs. 4c and 4d) has a modal value of the best fitting probability density function of ~~4~~ 5 m. By applying the same percentiles used for the hanging wall, a 90% cut off (FW90) was found at a distance of ~~~145~~ 265 m from the ~~main~~ principal fault. The FW75, FW50 and ~~FW40~~ FW35 correspond to distances of ~~~70~~ 120 m, ~~~25~~ 45 m and ~20 m from the ~~main~~ principal fault, respectively (Table 2a). It is worth noticing that also for the footwall the ~~40~~35% probability corresponds to a sharp drop of the data.~~bounds reasonably well the zone where the most of the ruptures occur.~~

The ratio between the width of the rupture zone on the footwall and the width of the rupture zone on the hanging wall ranges from 1:1.~~5~~ 8 to 1:2.2 (Table 2a), and therefore it is always close to 1:2 independently from the used percentile.

The results of the analysis performed on the entire database of distributed ruptures, including also the more complex secondary structures of B-M, F-S and Sy ruptures, is illustrated in Fig. 5 and summarized in Table 2b. As expected, the WRZ is significantly larger than for “simple thrust” distributed ruptures. The HW90, HW75 and HW50 correspond to distances of ~1100 m, ~640 m and ~260 m from the principal fault, respectively. For comparison with the “simple thrust” distributed ruptures, also the HW35 was calculated (~130 m), but it does not correspond with a particular drop of the data in the histogram of Fig. 5b. Instead, a sharp drop is visible at a distance of ~40 m from the principal fault, as for the “simple thrust” database. In the footwall, the FW90, FW75 and FW50 correspond to distances of ~720 m, ~330 m and ~125 m from the principal fault, respectively. The FW35 corresponds to a distance of ~65 m, but the sharp drop of the data in the histogram of Fig, 5d is at a distance of ~20 m from the principal fault, as for the “simple thrust” database.

In order to analyse the potential relationships between WRZ and the earthquake size, in Fig. ~~5~~ 6 the total width of the rupture zone (WRZ tot = WRZ hanging wall + WRZ footwall) is plotted against ~~the~~ Mw (Fig. 6a) and, for the subset of data having displacement information, against the vertical displacement (VD) on the principal fault (Fig. 6b).~~displacement on the main fault (vertical component, VD) for the subset of data having displacement information~~. The vertical displacement measured at the ground surface is highly sensitive to the shallow geometry of the thrust plane. The net displacement along the slip vector is a more appropriate parameter for considering the size of the displacement at the surface. However, the net displacement is rarely given in the literature, or can be obtained only by assuming a fault dip, while VD is the most commonly measured parameter. Therefore, we used VD as a proxy of the amount of surface displacement. In Fig. 6a a positive relation between the total WRZ and Mw is clear, particularly if sympathetic (Sy) fault ruptures are not considered. In fact, Sy data appear detached from the other data, suggesting that their occurrence is only partially dependent on the magnitude of the mainshock. They also depend on the structural features of the area, such as 1) whether or not an active, favourably-oriented fault is present, and 2) its distance from the main seismogenic source. ~~Though a broad positive~~A correlation between the total WRZ and VD ~~can be speculated, especially if the data with B-M and F-S faults is excluded, a clear correlation~~ is not obvious (Fig. ~~5a~~6b). Even for small values of VD (< 1 m) the total WRZ can be as wide as hundreds of meters, but a larger number of displacement data is necessary for drawing convincing conclusions. ~~A possible correlation can be found by zooming in the diagram in the area close to the main fault (WRZ <200 m, Fig. 5b). Close to the main fault (WRZ < 60 m), the width of the rupture zone appears to have a nearly linear upper boundary which correlates positively with VD, for VD < ~2 m (dashed line in Fig. 5b). This suggests that close to the main fault the width of the rupture zone increases with displacement, from a minimum of nearly 20 m for decimetric VD up to 50-60 m for VD close to 2 m. However, also for VD <2 m, the maximum WRZ, including the secondary ruptures away from the main fault, can be up to 200 m or wider.~~

4 Comparison with Italian guidelines and implications for fault zoning during seismic microzonation

The definition of the WRZ based on the analysis of the data from worldwide thrust earthquakes can support the evaluation and mitigation of SFRH. The values reported in Table 2 can be used for shaping and sizing fault zones (e.g. Warning or Susceptible Zones in the Italian guidelines; Earthquake Fault Zones in the A-P Act) and avoidance zones around the trace of active thrust faults (Table 3).

A first question that needs to be answered is which set of data between "simple thrust" distributed ruptures (Fig. 4; Table 2a) and all distributed ruptures (Fig. 5, Table 2b) is the most appropriate to be used for sizing the fault zones. The answer is not easy and implicates some subjective choices. In Table 3 we suggest using the results from "simple thrust" distributed ruptures. The results from all distributed ruptures can be used in areas with poor geologic knowledge, in order to assess the extent of the area within which potential sources of fault displacement hazard can be present. Our choices result from the following line of reasoning:

1) The data analysed in this work are from brittle rupture of the ground surface. The measured distributed ruptures are always associated with surface faulting on the principal fault. Therefore, the results can be used for zoning the hazard deriving from mechanisms connected with the propagation of the rupture on the main fault plane up to the surface. Deformations associated with blind thrusting are not analysed. Therefore, the results are not suitable for zoning ductile tectonic deformations associated with blind thrusting (e.g. folding). Clearly, coseismic folding occurs both during blind thrusting and surface faulting thrusting. Furthermore, brittle surface ruptures and other ductile deformations can be strictly connected to each other, making difficult to separate the two components, but a global analysis of the entire spectrum of permanent tectonic deformation associated to thrust faulting need additional data not considered here.

2) In most cases, distributed ruptures occur on secondary structures that are small and cannot be recognized before the earthquake, or that only site-specific investigations could distinguish. Fault zones should include the hazard from this kind of ruptures.

3) Some secondary faults connected with the principal fault can be sufficiently large to have their own geologic and geomorphic signature, and can be recognized before the earthquake. Most likely, close to the surface these structures behave similarly to the principal fault, with their own distributed ruptures. Faults with these characteristics should have their own zone, unless they are included in the principal fault zone.

4) Point 3 also applies to distant large active faults that can undergo sympathetic triggering. They should be zoned as separate principal faults. Using Sy ruptures for shaping zones of fault rupture hazard would imply distributing the hazard within areas that can be very large (Fig.s 5, 6). The size of the resulting zone would depend

mostly on the structural setting of the analysed areas (presence or not of the fault, distance from the seismogenic source) rather than the mechanics which controls distributed faulting in response to principal faulting.

5) B-M and F-S fault ruptures are not always present. Where present, they occur over distances ranging from hundreds of meters to kilometers (Fig. 3c). In any case, B-M and F-S secondary faults are strictly related to the structural setting of the area (large-scale folding; fold shape, wavelength and tightness; stiffness of folded strata). In fact, B-M fault ruptures commonly observed in historical earthquakes are normal faults. B-M normal faults are expected to occur in the shallowest convex (lengthened) layer of the folded anticline. They can occur only where the bending stress is tensional, that is the convex side of the folded layer, preferentially close to the crest of the anticline and parallel to the anticline hinge. F-S faults can rupture the surface where the steeply-dipping limb of a fold is formed by strata of stiff rocks able to slip along bedding planes (e.g. Fig. 2i). Moreover, it is known that coseismic B-M or F-S faults often reactivate pre-existing fault scarps (e.g. Yeats, 1986) which might help in zoning the associated potential fault rupture hazard before the earthquake. Therefore, knowledge of the structural setting of the area can help in identifying zones potentially susceptible to B-M or F-S faulting, which should be zoned as separate sources of fault rupture hazard.

In Table 3, the total WRZ from the present study is compared with the sizes of the zones proposed by the Italian guidelines for SM studies (Technical Commission for Seismic Microzonation, 2015; SM Working Group, 2015). The values reported in Table 3 ~~table~~ ~~can~~ could be used~~considered as a proposal~~ for integrating the existing criteria. In particular, the total WRZ from “simple thrust” distributed ruptures is used for sizing Warning Zones (Level 1 SM) and Susceptible and Avoidance Zones (Level 3 SM). The total WRZ from all distributed ruptures is suggested to be used for sizing Warning Zones in areas with poor basic geologic knowledge (Level 1 SM).

The first observation is that the FW:HW ratio proposed by the Italian guidelines is supported by the results of this study (FW:HW ratio close to 1:2).

Assuming that the 90% probability is a reasonable criterion for cutting the outliers from the analysed population, the resulting total WRZ (HW + FW) for “simple thrust” distributed ruptures is ~~465~~ 840 m (560 m on the HW + 280 m on the FW). This width could be used for zoning all the reasonably inferred fault rupture hazard, from both the ~~main~~ principal fault and ~~secondary~~ distributed ~~faults~~ruptures, during basic (Level 1) SM studies, which do not require high-level specific investigations. The obtained value is ~~not very~~significantly different from that recommended by the Italian guidelines for Level 1 SM (400 m).

~~The most~~A significant ~~evident~~ difference between our proposal and the Italian guidelines concerns also the width of the zone that should be avoided, due to the very high likelihood of having surface ruptures. Though the entire rupture zone could be hundreds of meters wide, ~~40-50% of~~more than one third of ~~secondary~~ distributed ruptures are expected to occur within a narrow, ~~50-7~~60 ~~m~~ m-wide zone. As could be expected, only site-specific paleo-sismologic investigations can quantify the hazard from surface faulting at a specific site. In the absence of such a detail, and for larger areas (e.g. municipality scale) the fault avoidance zone should be in the order of ~~50-7~~60 m, shaped asymmetrically compared to the trace of the main fault (~~30-45~~40 m on the HW; 20~~-25~~ m on the FW). ~~Figure 5b suggests a positive relation between the displacement on the main fault and the width of the rupture zone close to the main fault (WRZ ≤ 60 m). Assuming that this relation is real, Fig. 5b suggests that the avoidance zone should be larger than 20-30 m, even for displacements of a few decimetres.~~

In Table 3 a width of ~~210~~ 380 m is proposed for the susceptible zone (Level 3 SM). The choice of defining the width of the zone as the 3rd quartile (3 out of 4 probability that secondary faulting lies within the zone) is rather arbitrary. In fact, the width of the susceptible zone should be flexible. Susceptible zones are used only if uncertainties remain also after high-level seismic microzonation studies, such as uncertainties on the location of the main fault trace or about the possibility of secondary faulting away from the main fault. Susceptible zones can also be used for areas where a not better quantifiable distributed faulting might occur, such as in structurally complex zones (e.g. stepovers between main fault strands).

~~It is important to underline that the proposed criteria are applicable only to simple thrust ruptures, without B-M or F-S faults. B-M and F-S secondary faults are strictly related to the structural setting of the area (large-scale folding). Therefore, knowledge of the structural setting of the area may help in identifying zones potentially susceptible to B-M or F-S faulting. In fact, the B-M surface-ruptures commonly observed in historical earthquakes are normal faults. B-M normal faults are expected to occur in the shallowest convex (lengthened) layer of the folded anticline. They can occur only where the bending stress is tensional, that is the convex side of the folded layer, preferentially close to the crest of the anticline and parallel to the anticline hinge. F-S faults can rupture the surface where steeply-dipping limbs of folds associated to the seismogenic thrust, formed by stiff strata able to slip along bedding planes, intersect the topography (e.g. Fig. 2i). Thus, zones of potential B-M or F-S secondary faulting can be traced by knowing the geometry and wavelength of the fold and the first order stiffness of the folded material. Moreover, it is known that coseismic B-M or F-S faults often reactivate pre-existing fault scarps (e.g. Yeats, 1986) being the geomorphic signature which might help in zoning the associated SFRH.~~

5 Conclusions

The distribution of coseismic surface ruptures (distance of distributed~~secondary~~ ruptures from the ~~main~~ principal fault rupture) for ~~10~~ 11 well-documented historical surface faulting thrust earthquakes (5.4 ≤ M ≤ 7.9) provide constraints on the general characteristics of the surface rupture zone, with implications for zoning the surface rupture hazard along active thrust faults.

~~Secondary~~ Distributed ruptures can occur up to large distances from the ~~main~~ principal fault (~~~750 m on the footwall and ~1,600 m~~ up to ~3,000 m on the hanging wall), but most of them occur within few dozens of meters from the ~~main~~ principal fault. The distribution of secondary ruptures is asymmetric, with most of them located on the hanging wall. Coseismic folding of large-scale folds (hundreds of meters to kilometres in wavelength) may produce bending-moment (B-M) or flexural-slip (F-S) ~~secondary~~ fault ruptures on the hanging wall and footwall, respectively, widening significantly the rupture zone. Additional widening of the rupture zone can be due to sympathetic slip on distant active faults (Sy fault ruptures).

The distribution of secondary ruptures for "simple thrust" ruptures (without B-M, ~~and~~ F-S, and Sy fault ruptures) can be fitted by a continuous probability density function, of the same form for both the hanging wall and footwall. This function can be used for removing outliers from the ~~analyzed~~ analysed database (e.g. 90% probability) and define ~~cold~~ criteria for shaping SFRH zones. These zones can be used during seismic microzonation studies and can help in integrating existing guidelines.

~~The 90% probability of the cumulative distribution function defines a rupture zone of ~320 m-wide on the hanging wall and ~145 m-wide on the footwall (total width of ~465 m). This wide zone could be used for zoning SFRH during basic seismic microzonation studies (i.e. Level 1 SM according to the Italian guidelines), which typically lack of specific investigations and therefore are characterized by uncertainties on the location of the main fault and on the occurrence of secondary faulting away from the main fault.~~

More than ~~40-50%~~one third of the ruptures are expected to occur within a zone of ~60 ~~30-45~~ m-wide ~~on the hanging wall and 20-25 m-wide on the footwall (total width being 50-70 m)~~. This narrow zone could be used for defining the fault avoiding zone during high-level, municipality-scale seismic microzonation studies (i.e. Level 3 SM according to the Italian guidelines). The average FW:HW ratio of the WRZ -is close to 1:2, independently from the used percentile.

~~A possible positive relation between the displacement on the main fault and the total width of the rupture zone (total WRZ) is found only close to the main fault (total WRZ ≤ 60 m). Close to the main fault, the WRZ appears to increase with displacement, from a minimum of nearly 20-30 m for decimetric vertical displacement (VD) up~~

to 50-60 m for VD close to 2 m. This suggests that the avoidance zone should be larger than 20-30 m, even for displacements of a few decimetres.

The average FW:HW ratio of the WRZ is close to 1:2, independently from the used percentile.

In addition to the expected rupture zone along the trace of the main thrust, zones potentially susceptible to B-M or F-S secondary faulting can be inferred identified by detailed knowledge of the structural study setting of the area (shape, wavelength, tightnessgeometry, wavelength and lithology of the thrust-related large-scale folds) and by scrutinize possible geomorphic traces of past secondary faulting. Where recognized, these areas should have their own zones of fault rupture hazard.

The analysis of the entire database of distributed ruptures (Fig. 5) indicates significantly larger rupture zones compared to the database without B-M, F-S and Sy ruptures. This is due to the combination of processes related to the propagation up to the surface of the main fault rupture and other processes associated with large-scale co-seismic folding, as well as triggering of distant faults. These data can be useful in poorly-known areas, in order to assess the extent of the area within which potential sources of fault displacement hazard can be present.

The results from this study, particularly the function obtained in Fig. 4, can be used for improving the attenuation relationships for distributed faulting with distance from the principal fault, with possible applications in probabilistic studies of fault displacement hazard (e.g., Youngs et al., 2003; Petersen et al., 2011).

Competing interests

The authors declare that they have no conflict of interest.

Acknowledgements

The project was funded by Department DiSPUTer, “G. D’Annunzio” University of Chieti-Pescara (research funds to P. Boncio).

References

Angelier, J., Lee, J. C., Chu, H. T., and Hu, J. C.: Reconstruction of fault slip of the September 21st, 1999, Taiwan earthquake in the asphalted surface of a car park, and co-seismic slip partitioning, J. Struct. Geol., 25, 345-350, 2003.

Avouac, J. P., Ayoub, F., Leprince, S., Konea, O., and Helmberger, V.: The 2006 Mw 7.6 Kashmir earthquake: sub-pixel correlation of ASTER images and seismic waveforms analysis, Earth Planet. Sci. Lett., 249, 514-528, 2006.

Bilham, R. and Yu, T. T.: The morphology of thrust faulting in the 21 September 1999, Chichi, Taiwan earthquake, J. Asian Earth Sci., 18, 351-367, 2000.

Boncio, P., Galli, P., Naso, G., and Pizzi, A.: Zoning Surface Rupture Hazard along Normal Faults: Insight from the 2009 M_W 6.3 L'Aquila, Central Italy, Earthquake and Other Global Earthquakes, Bull. Seism. Soc. Am., 102, 918-935, doi: 10.1785/0120100301, 2012.

Bowman, J. R. and Barlow, B. C.: Surveys of the fault scarp of the 1986 Marryat Creek, South Australia, earthquake, [Australian] Bureau of Mineral Resources, Geology and Geophysics Record 1991/190, 12 pp., 3 plates, 1991.

Bryant, W. A. and Hart, E. W.: Fault-Rupture Hazard Zones in California, Alquist-Priolo Earthquake Fault Zoning Act With Index to Earthquake Fault Zones Maps, Calif Geol. Surv. Spec. Pub., 42, 41 pp, 2007.

Central Geological Survey, MOEA at http://gis.moeacgs.gov.tw/gwh/gsb97-1/sys8/index.cfm

Chang, J. C. and Yang, G. S.: Deformation and occurrence of the Che-lung-pu Fault from geomorphic evidence, Quat. Int., 115-116, 177-188, 2004.

Chen, C. H., Chou, H.S., Yang, C.Y., Shieh, B. J., and Kao, Y. H.: Chelungpu fault inflicted damages of pile foundations on FWY rout 3 and Fault zoning regulations in Taiwan, A Workshop on Seismic Fault-induced Failures, Tokyo, 2003.

Chen, G. H., Xu, X. W., Zheng, R. Z., Yu, G. H., Li, F., Li, C. X., Wen, X. Z., He, Y. L., Ye, Y. Q., Chen, X. C., and Wang, Z. C.: Quantitative analysis of the co-seismic surface rupture of the 2008 Wenchuan earthquake, Sichuan, China along the Beichuan-Yingxiu Fault, Seismol. Geol., 30 (3), 723-738, 2008 (in Chinese with English abstract).

Chen, W. C., Chu, H. T., and Lai, T. C.: Surface ruptures of the Chi-Chi Earthquake in the Shihgang Dam area, Special Issue for the Chi-Chi Earthquake, 1999, Special Publication of the Central Geological Survey, 12, 41-62, 2000 (in Chinese with English abstract).

Crone, A. J., Machette, M. N., and Bowman, J. R.: Geologic investigations of the 1988 Tennant Creek, Australia, earthquakes— Implications for paleoseismicity in stable continental regions, U.S. Geol. Surv. Bull. 2032-A, A1–A51, 1992.

Dong S, Zhang Y, Wu Z, Yang, N., Ma, Y., Shi, W., Chen, Z., Long, C., and An, M.: Surface Rupture and Co-seismic Displacement Produced by the Ms8.0 Wenchuan Earthquake of May 12th, 2008, Sichuan, China: Eastwards Growth of the Qinghai-Tibet Plateau, Acta Geol. Sin., 82 (5), 938-948, 2008a.

Dong, S., Han, Z., and An, Y.: Surface deformation at the epicenter of the May 12, 2008 Wenchuan M8 Earthquake, at Yingxiu Town of Sichuan Province, China, Sci. China Ser. E, 51, 154–163, doi:10.1007/s11431-008-6007-0, 2008b.

Faccioli, E., Anastasopoulos, I., Gazetas, G., Callerio, A., and Paolucci R.: Fault rupture–foundation interaction: selected case histories, Bull. Earthquake Eng., 6 (4), 557-583, 2008.

Fredrich, J., McCaffrey, R., and Denham, D.: Source parameters of seven large Australian earthquakes determined by body waveform inversion, Geoph. J., 95, 1-13, 1988.

Haessler, H., Deschamps, A., Dufumier, H., Fuenzalida, H. and Cisternas, A.: The rupture process of the Armenian earthquake from broad-band teleseismic body wave records, Geophys. J. lnt., 109, 151-161, 1992.

Huang, C., Chan, Y. C., Hu, J. C., Angelier, J., and Lee, J. C.: Detailed surface co-seismic displacement of the 1999 Chi-Chi earthquake in western Taiwan and implication of fault geometry in the shallow subsurface, J. Struct. Geol., 30, 1167-1176, 2008.

Huang, W. J., Chen, Z. Y., Liu, S. Y., Lin, Y. H., Lin, C. W., and Chang, H. C.: Surface deformation models of the 1999 Chi–Chi earthquake between Tachiachi and Toupienkengchi, central Taiwan, Special Issue for the Chi-Chi Earthquake, 1999, Special Publication of the Central Geological Survey, 12, 63–87, 2000 (in Chinese with English abstract).

Huang, W. J.: Deformation at the leading edge of thrust faults, Ph.D. dissertation, Purdue University, West Lafayette, Indiana, 435 pp., 2006.

Ishimura, D., Okada, S., Niwa, Y., and Toda, S.: The surface rupture of the 22 November 2014 Nagano-kenhokubu earthquake (Mw 6.2), along the Kamishiro fault, Japan, Active Fault Research, 43, 95-108, 2015 (in Japanese with English abstract).

Kaneda, H., Nakata, T., Tsutsumi, H., Kondo, H., Sugito, N., Awata, Y., Akhtar, S. S., Majid, A., Khattak, W., Awan, A. A., Yeats, R. S., Hussain, A., Ashraf, M., Wesnousky, S. G. and Kausar, A. B.: Surface rupture of the 2005 Kashmir, Pakistan, Earthquake and its active tectonic implications, Bull. Seismol. Soc. Am., 98, 521–557, 2008.

Kawashima, K.: Damage of bridges resulting from fault rupture in the 1999 Kocaeli and Dunce, Turkey earthquakes and the 1999 Chi-Chi, Taiwan earthquake, Structural Engineering/Earthquake Engineering, 19(2), 179s–197s, 2002.

Kelson, K. I., Kang, K. H., Page, W. D., Lee, C. T., and Cluff, L. S., 2001: Representative styles of deformation along the Chelungpu Fault from the 1999 Chi-Chi (Taiwan) earthquake: geomorphic characteristic and responses of man-made structures, Bull. Seismol. Soc. Am., 91(5), 930–952, 2001.

Kelson, K. I., Koehler, R. D., Kang, K.-H., Bray, J. D. and Cluff, L. S.: Surface deformation produced by the 1999 Chi-chi (Taiwan) earthquake and interactions with built structures, Final Technical Report, U.S.G.S. Award No. 01-HQ-GR-0122, 21 pp., 2003.

Kerr, J., Nathan, S., Van Dissen, R., Webb, P., Brunsdon, D., and King, A.: Planning for development of land on or close to active faults: A guide to assist resource management planners in New Zealand. Report prepared for the Ministry for the Environment by the Institute of Geological & Nuclear Sciences, Client Report 2002/124, Project Number 440W3301, 2003.

Konagai, K., Hori, M., Meguro, K., Koseki, J., Matsushima, T., Johansson, J., and Murata, O.: Key Points for Rational Design for Civil Infrastructures near Seismic Faults Reflecting Soil-Structure Interaction Features, Report of JSPS research project, grant-in-aid for scientific research (A) Project No.16208048, 2006.

Kumahara, Y. and Nakata, T.: Recognition of active faults generating the 2005 Pakistan earthquake based on interpretation of the CORONA satellite photographs, E-journal GEO, 2 (2), 72-85, 2007 (In Japanese with English abstract).

Lee, G. C. and Loh, C. H. (Eds): The Chi-Chi, Taiwan Earthquake of September 21, 1999: Reconnaissance Report, Technical Report MCEER-00-0003 April 30, 2000.

Lee, J. C. and Chan, Y. C.: Structure of the 1999 Chi-Chi earthquake rupture and interaction of thrust faults in the active fold belt of western Taiwan, J. Asian Earth Sci., 31, 226-239, 2007.

Lee, J. C., Chen, Y. G., Sieh, K., Mueller, K., Chen, W. S., Chu, H. T., Chan, Y. C., Rubin, C., and Yeats, R.: A Vertical Exposure of the 1999 Surface Rupture of the Chelungpu Fault at Wufeng, Western Taiwan: Structural and Paleoseismic Implications for an Active Thrust Fault, Bull. Seismol. Soc. Am., 91, 5, pp. 914-929, 2001.

Lee, Y. H., Hsieh, M. L., Lu, S. D., Shih, T. S., Wu, W. Y., Sugiyama, Y., Azuma, T., and Kariya, Y.: Slip vectors of the surface rupture of the 1999 Chi-Chi earthquake, western Taiwan, J. Struct. Geol., 25, 1917-1931, 2003.

Lee, Y. H., Wu, K. C., Rau, R. J., Chen, H. C., Lo, W., and Cheng, K. C.: Revealing coseismic displacements and the deformation zones of the 1999 Chi-Chi earthquake in the Tsaotung area, central Taiwan, using digital cadastral data, J. Geophys. Res., 115, B03419, 2010.

Lettis, W. R., Wells, D. L., and Baldwin, J. N.: Empirical observations regarding reverse earthquakes, blind thrust faults, and quaternary deformation: Are blind thrust faults truly blind?, Bull. Seismol. Soc. Am., 87(5), 1171–1198, 1997.

Lin, A., Sano, M., Yan, B., and Wang, M.: Co-seismic surface ruptures produced by the 2014 Mw 6.2 Nagano earthquake, along the Itoigawa–Shizuoka tectonic line, central Japan, Tectonophysics, 656, 142-153, 2015.

Lin, W. H.: On surface deformations from the Chi-Chi earthquake in the Shihkang and Chutzekeng areas, Special Issue for the Chi-Chi Earthquake, 1999, Special Publication of the Central Geological Survey, 12, 1-17, 2000 (in Chinese with English abstract).

Liu-Zeng, J., Sun, J., Wang, P., Hudnut, K. W., Ji, C., Zhang, Z., Xu, Q., and Wen, L.: Surface ruptures on the transverse Xiaoyudong fault: A significant segment boundary breached during the 2008 Wenchuan earthquake, China, Tectonophysics 580, 218–241, 2012.

Liu-Zeng, J., Sun, J., Zhang, Z., Wen, L., Xing, X., Hu, G., and Xu, Q.: Detailed mapping of surface rupture of the Wenchuan Ms 8.0 earthquake near Hongkou and seismotectonic implications, Quaternary Sciences, 30 (1), 1-29, 2010 (in Chinese with English abstract).

Liu-Zeng, J., Zhang, Z., Wen, L., Tapponnier, P., Sun, J., Xing, X., Hu, G., Xu, Q., L. Zeng, L., Ding, L., Ji, C., Hudnut, K.W., and van der Woerd, J.: Co-seismic ruptures of the 12 May 2008, Ms 8.0 Wenchuan earthquake, Sichuan: East–west crustal shortening on oblique, parallel thrusts along the eastern edge of Tibet, Earth Plan. Sci. Lett., 286, 355-370, 2009.

Machette, M. N., Crone, A. J., and Bowman, J. R.: Geologic investigations of the 1986 Marryat Creek, Australia, earthquakes - implications for paleoseismicity in stable continental regions, U.S. Geol. Sur. Bull. 2032-B, 29, 1993.

McCaffrey, R.: Teleseismic investigation of the January 22, 1988 Tennant Creek, Australia, earthquakes, Geophys. Res. Lett., 16, 413-416, 1989.

Meghraoui, M., Jaegy, R., Lammali, K., and Albarède, F.: Late Holocene earthquake sequences on the El Asnam (Algeria) thrust fault, Earth Planet. Sci. Lett., 90, 187–203, 1988.

Okada, S., Ishimura, D., Niwa, Y., and Toda, S.: The First Surface-Rupturing Earthquake in 20 Years on a HERP Active Fault is Not Characteristic: The 2014 Mw 6.2 Nagano Event along the Northern Itoigawa–Shizuoka Tectonic Line, Seismol. Res. Lett., 86 (5), 1–14, 2015.

Ota, Y., Huang, C. Y., Yuan, P. B., Sugiyama, Y., Lee, Y. H., Watanabe, M., Sawa, H., Yanagida, M., Sasaki, S., Suzuki, Y., Tang, H. S., Shu, U.T., Yang, S. Y., Hirouchi, D., and Taniguchi, K.: Trenching Study at the

Tsautun Site on the Central Part of The Chelungpu Fault, Taiwan, J. Geogr., 110 (5), 698-707, 2001 (in Japanese with English abstract).

Ota, Y., Shishikura, M., Ichikawa, K., Watanabe, M., Yanagida, M., Tanaka, T., Sawa, H., Yamaguchi, M., Lee, Y. H., Lu, S. T., Shih, T. S., and Amagasa, S.: Low-angle reverse faulting during two earthquakes on the northern part of the Chelungpu fault, deduced from the Fengyuan trench, Central Taiwan, Terr. Atmos. Ocean. Sci., v. 18, no. 1, p. 55–66, 2007b.

Ota, Y., Watanabe, M., Suzuki, Y., Yanagida, M., Miyawaki, A., and Sawa, H.: Style of the surface deformation by the 1999 Chichi earthquake at the central segment of Chelungpu fault, Taiwan, with special reference to the presence of the main and subsidiary faults and their progressive deformation in the Tsauton area, J. Asian Earth Sci., 31, 214-225, 2007a.

Petersen, M., Dawson, T.E., Chen, R., Cao, T., Wills, C.J.,Schwartz, D.P., and Frankel, A.D.: Fault displacement hazard for strike-slip faults, Bull. Seismol. Soc. Am, 101 (2), 805–825, 2011.

Philip, H. and Meghraoui, M.: Structural analysis and interpretation of the surface deformation of the El Asnam earthquake of October 10, 1980, Tectonics, 2, 17-49, 1983.

Philip, H., Rogozhin, E., Cisternas, A., Bousquet, J. C., Borisov, B., and Karakhanian, A.: The Armenian earthquake of 1988 December 7: faulting and folding, neotectonics and palaeoseismicity, Geophys. J. Int., 110, 141-158, 1992.

Rajendran, C. P., Rajendran, K., Unnikrishnan, K. R., and John, B.: Palaeoseismic indicators in the rupture zone of the 1993 Killari (Latur) earthquake, Curr. Sci., 70 (5), 385-390, 1996.

Rymer, M. J., Kendrick, K. J., Lienkaemper, J. J., and Clark, M. M.: Surface rupture on the Nunez fault during the Coalinga earthquake sequence, in Rymer, M.J, and Ellsworth, W.L. eds., The Coalinga, California, Earthquake of May 2, 1983, U.S. Geol. Sur. Prof. Paper 1487, 299-318, 1990.

Sayab, M. and Khan, M.A.: Temporal evolution of surface rupture deduced from coseismic multi-mode secondary fractures: Insights from the October 8, 2005 (Mw 7.6) Kashmir earthquake, NW Himalaya, Tectonophysics, 493, 58–73, 2010.

Seeber, L., Ekstrom, G., Jain, S.K., Murty, C.V.R., Chandak, N., and Armbruster, J. G.: The 1993 Killari earthquake in central India: a new fault in Mesozoic basalt flows?, J. Geophys. Res., 101, 8543-8560, 1996.

Shin, T. C. and Teng, T. L.: An overview of the 1999 Chi-Chi, Taiwan, Earthquake, Article in Bull. Seismol. Soc. Am., 91(5), 895-913, 2001

SM Working Group: Guidelines for Seismic Microzonation, Conference of Regions and Autonomous Provinces of Italy, Civil Protection Department, English edition of: Gruppo di lavoro MS, Indirizzi e criteri per la microzonazione sismica, Conferenza delle Regioni e delle Province autonome – Dipartimento della protezione civile, Roma, 2008, 3 vol. e Dvd, 2015. Available online at http://www.protezionecivile.gov.it/httpdocs/cms/attach_extra/GuidelinesForSeismicMicrozonation.pdf, 2015.

Technical Commission for Seismic Microzonation: Linee guida per la gestione del territorio in aree interessate da Faglie Attive e Capaci (FAC), versione 1.0, Conferenza delle Regioni e delle Province Autonome – Dipartimento della Protezione Civile, 55 pp., Roma, 2015 (In Italian).

Tsutsumi, H. and Yeats, R.: Tectonic setting of the 1971 Sylmar and 1994 Northridge earthquakes in the San Fernando valley, California, Bull. Seism. Soc Am., 89 (5), 1232-1249, 1999.

U.S. Geological Survey Staff: Surface faulting, in: The San Fernando, California, earthquake of February 9, 1971, U.S. Geol. Sur. Prof. Paper 733, 55-76, 1971.

Wang, H., Ran, Y, Chen, L., Shi, X., Liu, R., and Gomez, F.:Determination of horizontal shortening and amount of reverse-faulting from trenching across the surface rupture of the 2008 Mw 7.9 Wenchuan earthquake, China, Tectonophysics, 491, 10–20, 2010.

Wells, D. and Coppersmith, K.: New empirical relationships among magnitude, rupture length, rupture width, rupture area, and surface displacement, Bull. Seismol. Soc. Am., 84 (4), 974-1002, 1994.

Wesnousky, S. G.: Displacement and geometrical characteristics of earthquake surface ruptures: Issues and implications for seismic hazard analysis and the earthquake rupture process, Bull. Seismol. Soc. Am., 98(4), 1609–1632, 2008.

Xu, X., Wen, X., Ye, J., Ma, B., Chen, J., Zhou, R., He, H., Tian, Q., He, Y., Wang, Z., Sun, Z., Feng, X., Yu, G., Chen, L., Chen, G., Yu, S., Ran, Y., Li, X., Li, C., and An, Y.: The Ms 8.0 Wenchuan earthquake surface ruptures and its seismogenic structure, Seismol. Geol., 30 (3), 597-629, 2008 (in Chinese with English abstract).

Xu, X., Wen, X., Yu, G., Chen, G., Klinger, Y., Hubbard, J., and Shaw, J.: Co-seismic reverse- and oblique-slip surface faulting generated by the 2008 Mw 7.9 Wenchuan earthquake, China, Geology 37(6), 515–518, doi 10.1130/G25462A.1., 2009.

Yeats, R. S.: Active Faults Related to Folding, In Active Tectonics: Impact on Society, The National Academies Press, 280 pp., https://doi.org/10.17226/624, 1986.

Yelding, G., Jackson, J. A., King, G. C. P., Sinvhal H., Vita-Finzi, C., Wood, R. M.: Relations between surface deformation, fault geometry, seismicity, and rupture characteristics during the El Asnam (Algeria) earthquake of the 10 October 1980, Earth Planet. Sci. Lett., 56, 287-304, 1981.

Youngs, Y., W. J. Arabasz, R. R., Anderson, R. E., Ramelli, A. R., Ake, J. P., Slemmons, D. B., McCalpin, J. P., Doser, D. I., Fridrich, C. J., Swan III, F. H., Rogers, A. M., Yount, J. C., Anderson, L. W., Smith, K.

D.,Bruhn, R. L., Knuepfer, L. K., Smith, R. B., dePolo, C. M.,.O'Leary, K.W, Coppersmith, K. J., Pezzopane, S. K., Schwartz, D. P., Whitney, J. W., Olig, S. S., and Toro, G. R.: A methodology for probabilistic fault displacement hazard analysis (PFDHA), Earthq. Spectra 19, 191–219, 2003.

Yu, G. H., Xu, X. W., Chen, G. H., Gou, T. T., Tan, X. B., Yang, H., Gao, X., An, Y. F., and Yuan, R. M.: Relationship between the localization of surface ruptures and building damages associated with the Wenchuan 8.0 earthquake, Chinese J. Geophysics, Vol. 52, No. 6, pp. 1294-1311, 2009.

Yu, G., Xu, X., Klinger, Y., Diao, G., Chen, G., Feng, X., Li, C., Zhu, A., Yuan, R., Guo, T., Sun, X., Tan, X., and An, Y.: Fault-Scarp Features and Cascading-Rupture Model for the Mw 7.9 Wenchuan Earthquake, Eastern Tibetan Plateau, China, Bull. Seismol. Soc. Am., Vol. 100, No. 5B, pp. 2590-2614, 2010.

Zhang, J. Y., Bo, J. S., Xu, G. D., and Huang, J. Y.: Buildings Setbacks Research From Surface-Fault-Rupture Statistical Analysis, Applied Mechanics and Materials, Vols. 204-208, pp. 2410-2418, 2012.

Zhang, Y. S., Shi, J. S., Sun, P., Yang, W., Yao, X., Zhang, C. S., and Xiong T. Y.: Surface ruptures induced by the Wenchuan earthquake: Their influence widths and safety distances for construction sites, Eng. Geol. 166, 245–254, 2013.

Zhang, Y. S., Sun, P., Shi, J. S., Yao, X., and Xiong, T. Y.: Investigation of rupture influenced zones and their corresponding safe distances for reconstruction after 5.12 Wenchuan earthquake, Eng. Geol., 18 (3), 312-319, 2010 (in Chinese with English abstract).

Zhou, Q., Xu, X., Yu, G., Chen, X., He, H., and Yin, G.: Width Distribution of the Surface Ruptures Associated with the Wenchuan Earthquake: Implication for the Setback Zone of the Seismogenic Faults in Post-earthquake Reconstruction, Bull. Seismol. Soc. Am., Vol. 100, No. 5B, pp. 2660-2668, 2010.

Table 1. Earthquakes used for analysing the width of the rupture zone (WRZ).

Earthquake	Date	Magnitude	Kin. #	SRL* (km)	MD* (m)	Depth (km)	References for earthquake parameters (a) and WRZ calculation (b)
1) San Fernando, CA, USA	1971.02.09	M_s 6.5, M_w 6.6	R-LL	16	2.5	8.9 (USGS)	a) 1 b) 2
2) El Asnam, Algeria	1980.10.10	M_s 7.3, M_w7.1	R	31	6.5	10 (USGS)	a) 1 b) 3, 4, 5
3) Coalinga (Nunez), CA, USA	1983.06.11	M_s5.4, M_w 5.4	R	3.3	0.64	2.0 (USGS)	a) 1 b) 6
4) Marryat Creek, Australia	1986.03.30	M_s 5.8, M_w 5.8	R-LL	13	1.3	3.0	a) 1, 7 b) 8, 9
5) Tennant Creek, Australia	1988.01.22 (3 events)	M_s 6.3, M_w 6.3 M_s 6.4, M_w 6.4 M_s 6.7, M_w 6.6	R R-LL R	10.2 6.7 16	1.3 1.17 1.9	2.7 3.0 4.2	a) 1, 10 b) 11
6) Spitak, Armenia	1988.12.07	M_s 6.8, M_w 6.8	R-RL	25	2.0	5.0-7.0	a) 1, 12 b) 13
7) Killari, India	1993.09.29	M_s 6.4, M_w 6.2	R	5.5	0.5	2.6	a) 14, 15 b) 15, 16
8) Chi Chi, Taiwan	1999.09.20	M_w 7.6	R-LL	72	12.7	8.0	a) 17, 18 b) 19, 20, 21, 22, 23, 24, 25, 26, 27, 28, 29, 30, 31, 32, 33, 34, 35, 36, 37, 38, 39, 40, 41
9) Kashmir, Pakistan	2005.10.08	M_w 7.6	R	70	7.05 (v)	<15.0	a) 42, 43 b) 43, 44
10) Wenchuan, China	2008.05.12	M_w 7.9	R-RL	240	6.5 (v) 4.9 (h)	19.0 (USGS)	a) 45 b) 46, 47, 48, 49, 50, 51, 52, 53, 54, 55, 56, 57, 58, 59
11) Nagano, Japan	2014.11.22	M_w 6.2	R	9.3	1.5 (v)	4.5	a) 60, 62 b) 60, 61, 62

Commento [UW1]: New data

Kin. (kinematics): R = reverse, LL = left lateral, RL = right lateral.

* SRL = surface rupture length; MD = maximum displacement (vector sum, unless otherwise specified; v = vertical; h = horizontal).

References: 1 = Wells and Coppersmith, 1994; 2 =U.S. Geological Survey Staff, 1971; 3 =Yelding et al., 1981; 4 =Philip and Meghraoui, 1983; 5 =Meghraoui et al 1988; 6 = Rymer et al. 1990; 7 = Fredrich et al., 1988; 8 = Bowman and Barlow, 1991; 9 = Machette et al., 1993; 10 = McCaffrey, 1989; 11 = Crone et al., 1992; 12 = Haessler et al. 1992; 13 = Philip et al. 1992; 14 = Lettis et al., 1997; 15 = Seeber et al. 1996; 16 = Rajendran et al., 1996; 17 = Wesnousky 2008; 18 = Shin and Teng, 2001; 19 = Kelson et al., 2001; 20 = Kelson et al., 2003; 21 = Angelier et al., 2003; 22 = Bilham and Yu, 2000; 23 = Chang and Yang, 2004; 24 = Chen et al., 2000; 25 = Chen et al., 2003; 26 = Faccioli et al., 2008; 27 = Huang et al., 2008; 28 = Huang et al., 2000; 29 = Huang, 2006; 30 = Kawashima, 2002; 31 = Konagai et al., 2006; 32 = Lee and Loh, 2000; 33 = Lee et al., 2001; 34 = Lee and Chan, 2007; 35 = Lee et al., 2003; 36 = Lee et al., 2010; 37 = Lin, 2000; 38 = Ota et al., 2001; 39 = Ota et al., 2007a; 40 = Ota et al., 2007b; 41 = Central Geological Survey, MOEA at http://gis.moeacgs.gov.tw/gwh/gsb97-1/sys8/index.cfm; 42 = Avouac et al., 2006; 43 = Kaneda et al., 2008; 44 = Kumahara and Nakata, 2007; 45 = Xu et al., 2009; 46 = Liu-Zeng et al., 2009; 47 = Liu-Zeng et al., 2012; 48 = Yu et al., 2009; 49 = Yu et al., 2010; 50 = Zhou et al., 2010; 51 = Zhang et al., 2013; 52 = Chen et al., 2008; 53 = Dong et al., 2008a; 54 = Dong et al., 2008b; 55 = Liu-Zeng et al., 2010; 56 = Wang et al., 2010; 57 = Xu et al., 2008; 58 = Zhang et al., 2012; 59 = Zhang et al., 2010; 60 = Okada et al., 2015; 61 = Ishimura et al., 2015; 62 = Lin et al., 2015.

Table 2 - Width of the rupture zone (WRZ) on the hanging wall (HW) and on the footwall (FW) and FW to HW ratio for (a) "simple thrust" distributed ruptures (B-M, F-S and Sy excluded) and (b) all distributed ruptures.

(a)

Probability[1]	WRZ **HW**	WRZ **FW**	**Total** WRZ	**FW:HW**
90%	575 m	265 m	840 m	1:2.2
75%	260 m	120 m	380 m	1:2.2
50%	80 m	45 m	125 m	1:1.8
35%[2]	40 m	20 m	60 m	1:2

(b)

Probability[1]	WRZ **HW**	WRZ **FW**	**Total** WRZ	**FW:HW**
90%	1100 m	720 m	1820 m	1:1.5
75%	640 m	330 m	970 m	1:1.9
50%	260 m	125 m	385 m	1:2.1
35%[3]	130 m	65 m	195 m	1:2

Commento [UW2]: New table

[1] Probabilities refer to the cumulative distribution functions of Fig.s 4 and 5.
[2] Corresponding to a sharp drop of data in the histograms of Fig. 4, close to the principal fault.
[3] Calculated for comparison with "simple thrust" database, but not corresponding to particular drops of data in the histograms of Fig. 5.

Table 3 Comparison between fault zone size from Italian guidelines and the Width of the Rupture Zone (WRZ) from the present study (proposal for integrating fault zoning for thrust faults). PF = principal fault rupture; DR = distributed ruptures; SFRH = surface fault rupture hazard.

ZONE[1]	**Seismic Microzonation[2]**	**Italian guidelines**	**Proposed widths of zones from total WRZ (from "simple thrust" DR[3])**	**Total WRZ from all DR (including B-M, F-S and Sy)**	**FW:HW[5]**
Warning Zone (*Zona di attenzione, ZA*)	Basic (Level 1)	400 m (FW:HW = 1:2)	**> 380 m** (minimum; 75% prob.) to **840 m** (recommended; 90% prob., all the reasonably inferred hazard from PF and DR)	**1800 m** (90% prob., applicable in poorly-known areas for assessing the extent of potential SFRH)	1:2
Avoidance Zone (*Zona di rispetto*, ZR)	High-level (Level 3)	30 m (FW:HW = 1:2)	**60 m** (35% prob.[4], very high hazard)		1:2
Susceptible Zone (*Zona di suscettibilità*, ZS)	High-level (Level 3)	160 m (FW:HW = 1:2)	**Variable** (depending on the detail of Level 3 MS and structural complexity) **380 m** (in the absence of particular constraints; 75% prob., precautionary)		1:2

[1] The original names of zones in the Italian guidelines (in Italian) are in italics.
[2] Different levels of Seismic Microzonation refer to SM Working Group (2015).
[3] B-M, F-S and Sy fault ruptures are not included.
[4] Corresponding to a sharp drop of data in the histograms of Fig. 4.
[5] The computed values (Table 2) have been simplified to 1:2.

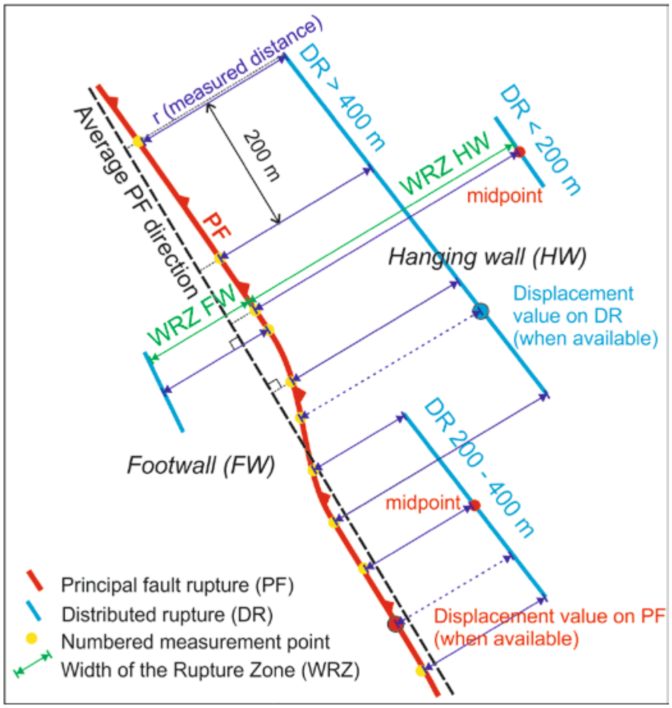

Figure 1 Sketch synthesizing the methodology used for measuring the "r" and WRZ data. Distance between the principal fault rupture and distributed rupture is measured along the line perpendicular to the auxiliary line indicating the average direction of the principal fault, always between the faults. Points with displacement values are prioritised at the expense of the 200 m metrics (the closest measurement point) when reasonable, in order to avoid over measuring.

Commento [UW3]: Update figure

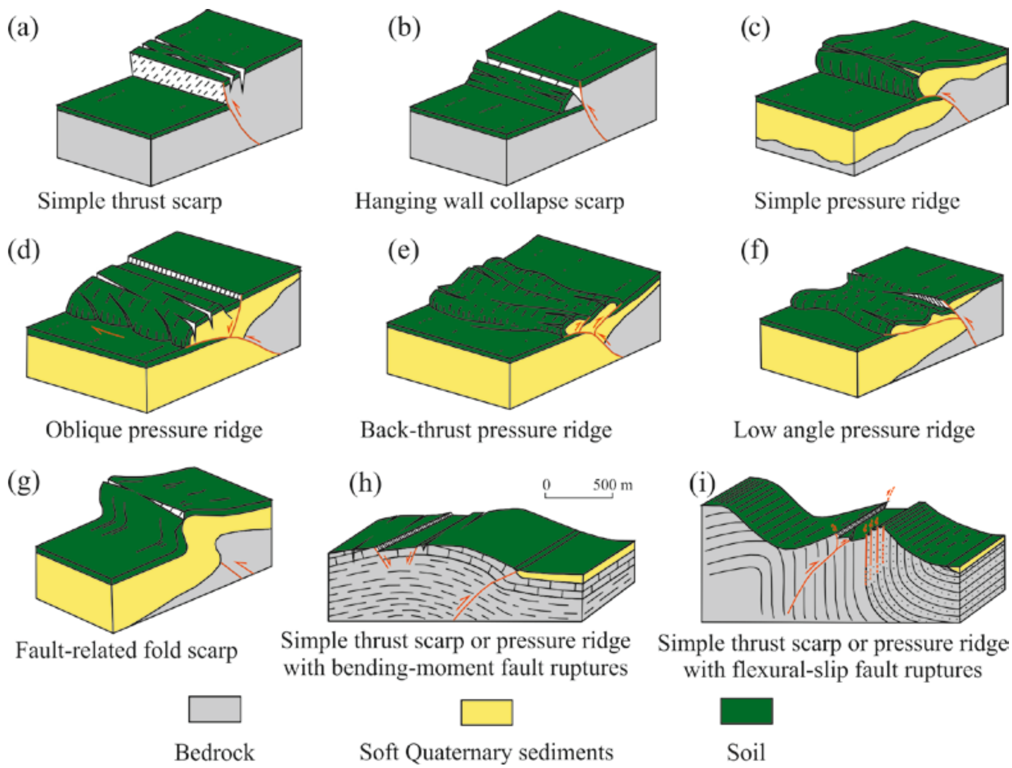

Figure 2 Scarp type classification (modified after Philip et al., 1992 and Yu et al., 2010). The scarp types h) and i) are associated with large-scale folds (hundreds of meters to kilometres in wavelength) and are from Philip and Meghraoui (1983).

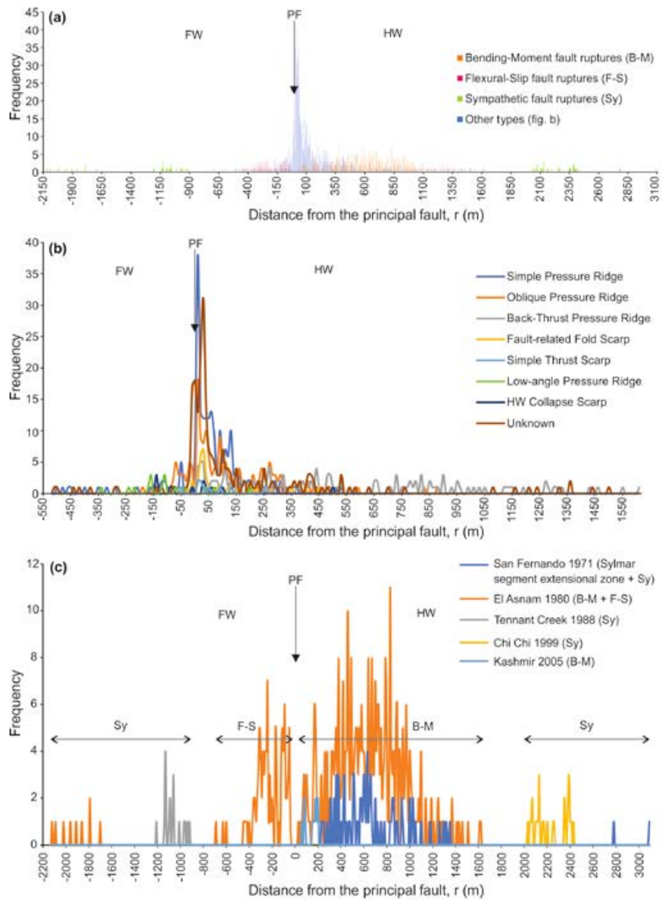

Figure 3 a) Frequency distribution histogram of the distributed ruptures distance (r) from the principal fault rupture (PF) for the earthquakes reported in Table 1. The positive and negative values refer to the data on the hanging wall and the footwall, respectively; b) Frequency distribution curves of each scarp type excluding those associated with B-M, F-S and Sy fault ruptures (types h and i of Fig. 2 and sympathetic slip triggered on distant faults); c) Frequency distribution curves of the B-M, F-S and Sy fault ruptures distinguished by earthquakes (the Sylmar segment extensional zone of the San Fernando 1971 earthquake rupture is included into the B-M fault ruptures).

Commento [UW4]: Updated figure

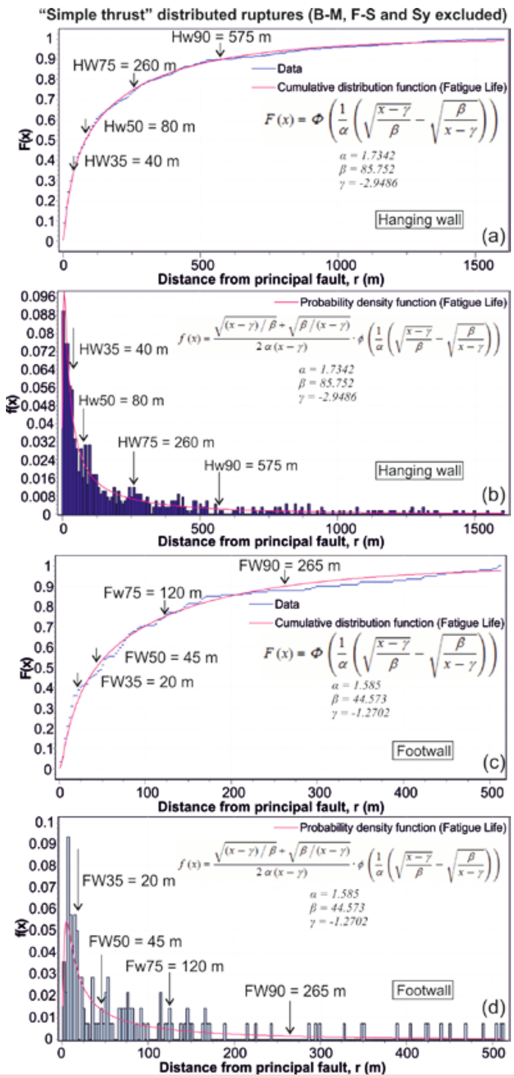

Figure 4 Cumulative distribution function and probability density function of the rupture distance (r) from the PF for the hanging wall (a and b, respectively) and the footwall (b and c, respectively) of the PF. Only the scarp types without associated B-M, F-S or sympathetic fault ruptures ("simple thrust" distributed ruptures) were analysed. The 35% probability (HW35) is indicated because it corresponds to sharp drop of the data in the histograms.

Commento [UW5]: Updated figure

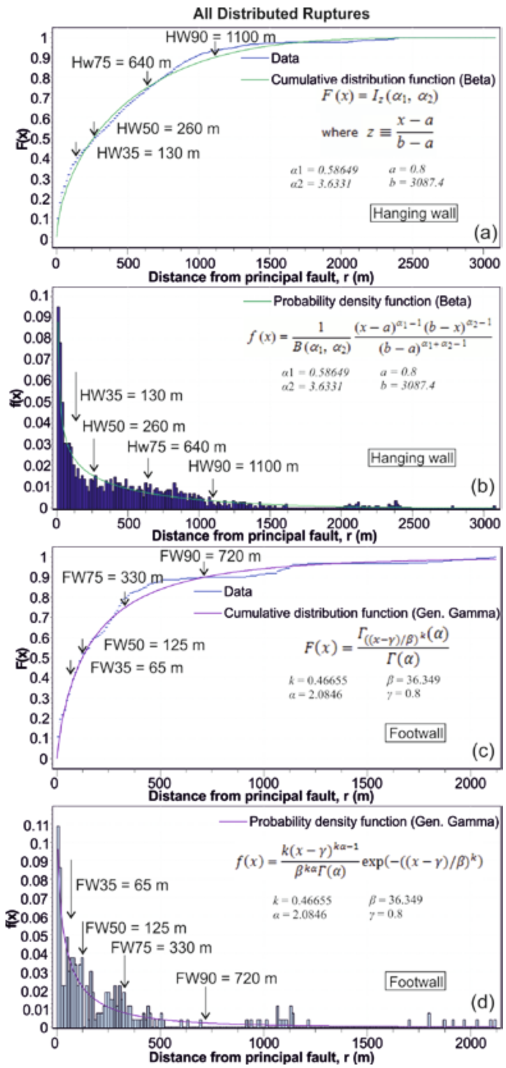

Figure 5 Cumulative distribution function and probability density function of the rupture distance (r) from the PF for the hanging wall (a and b, respectively) and the footwall (c and d, respectively) of the PF. All types of distributed ruptures were considered. The 35% probability (HW35) is indicated for comparison with "simple thrust" database (Fig. 4), but it does not correspond to particular drops of the data in the histograms.

Commento [UW6]: New figure

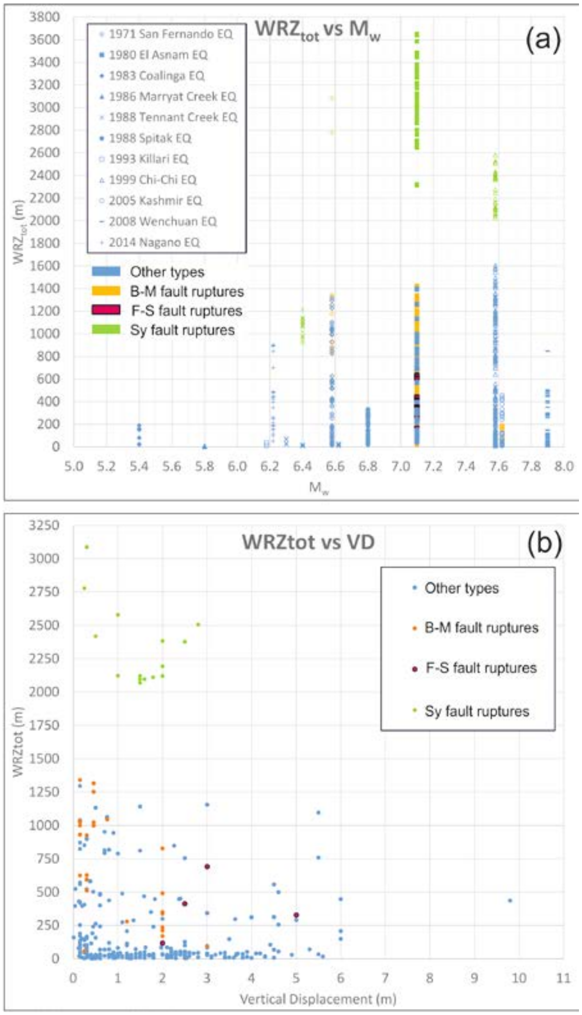

Figure 6 a) Diagram plotting the total WRZ (WRZtot = WRZ hanging wall + WRZ footwall) against (a) the earthquake magnitude (Mw) and (b) the vertical displacement (VD) on the principal fault.

Commento [UW7]: Modified figure